AN INVESTIGATION OF ACCURACY OF INERTIAL INTERACTION ANALYSES WITH FREQUENCY-INDEPENDENT IMPEDANCE COEFFICIENTS

A THESIS SUBMITTED TO
THE GRADUATE SCHOOL OF NATURAL AND APPLIED SCIENCES
OF
MIDDLE EAST TECHNICAL UNIVERSITY

BY

ÖZGÜN YILMAZOK

IN PARTIAL FULFILLMENT OF THE REQUIREMENTS
FOR
THE DEGREE OF MASTER OF SCIENCE
IN
CIVIL ENGINEERING

NOVEMBER 2007

Approval of the thesis:

AN INVESTIGATION OF ACCURACY OF INERTIAL INTERACTION ANALYSES WITH FREQUENCY-INDEPENDENT IMPEDANCE COEFFICIENTS

Submitted by **Özgün YILMAZOK** in partial fulfillment of the requirements for the degree of **Master of Science in Civil Engineering Department, Middle East Technical University** by,

Prof. Dr. Canan Özgen
Dean, Graduate School of **Natural and Applied Sciences** _____

Prof. Dr. Güney Özcebe
Head of Department, **Civil Engineering** _____

Assoc. Prof. Dr. Bahadır Sadık Bakır
Supervisor, **Civil Engineering, METU** _____

Asst. Prof. Dr. Mustafa Tolga Yılmaz
Co-supervisor, **Engineering Sciences, METU** _____

Examining Committee Members:

Prof. Dr. Mehmet Polat Saka
Engineering Sciences, METU _____

Assoc. Prof. Dr. Bahadır Sadık Bakır
Civil Engineering, METU _____

Assoc. Prof. Dr. Ahmet Yakut
Civil Engineering, METU _____

Asst. Prof. Dr. Mustafa Tolga Yılmaz
Engineering Sciences, METU _____

Asst. Prof. Dr. Murat Altuğ Erberik
Civil Engineering, METU _____

Date: 15.11.2007

I hereby declare that all information in this document has been obtained and presented in accordance with academic rules and ethical conduct. I also declare that, as required by these rules and conduct, I have fully cited and referenced all material and results that are not original to this work.

Özgün YILMAZOK

Signature:

ABSTRACT

AN INVESTIGATION OF ACCURACY OF INERTIAL INTERACTION ANALYSES WITH FREQUENCY-INDEPENDENT IMPEDANCE COEFFICIENTS

Yılmazok, Özgün

M.S., Department of Civil Engineering

Supervisor: Assoc. Prof. Dr. B. Sadık Bakır

November 2007, 79 pages

The inertial interaction between the soil and structure alters dynamic response characteristics of a structure due to foundation deformability, such that the flexibility and energy dissipation capability of surrounding soil may lead to a significant increase in period and damping of structural oscillations. The inertial interaction analyses can be accomplished through utilisation of frequency dependent foundation impedance coefficients that are reported in literature for various soil conditions and foundation types. However, such analyses should be performed in frequency domain, and applicable to only cases that linear structural response is considered. Alternatively, equivalent frequency-independent foundation impedance coefficients can be employed, such that a constant excitation frequency is assumed in calculation of these coefficients.

In this study, it is assumed that the fundamental frequency of a fixed-base structure, which can be obtained through employing available empirical relationships or a modal analysis, can be substituted for excitation terms in impedance expressions. The error induced in calculation of peak structural distortions is investigated through comparisons of structural response due to

frequency-dependent and frequency-independent foundation impedance coefficients. For analyses, a linear single-degree of freedom oscillator is considered for modeling the structure. The frequency-dependent impedance of a rigid disk foundation resting on elastic halfspace is simulated by a limited number of discrete elements. The response calculations are performed in frequency domain, through employing 72 acceleration records.

It is concluded that, the natural frequency of fixed-base building can be considered as effective excitation frequency for calculation of foundation impedance coefficients, when the effect of inertial interaction on structural response is moderate. Through employing equivalent-linear approximation for the structural response, it is shown that the conclusion is also valid in cases that nonlinear structural response is considered. However, when the inertial interaction has more profound effects on the structural response, the use of natural frequency of flexible-base structure, which is calculated iteratively due to its dependence on foundation-impedance factors is recommended.

Keywords: Soil-structure interaction, inertial interaction, foundation impedance

ÖZ

FREKANS-BAĞIMSIZ EMPEDANS KATSAYILARI İLE YAPILAN ATALET ETKİLEŞİMİ ANALİZLERİNİN DOĞRULUĞU ÜZERİNE BİR İNCELEME

Yılmazok, Özgün

Yüksek Lisans, İnşaat Mühendisliği Bölümü

Tez Yöneticisi: Prof. Dr. B.Sadık Bakır

Kasım 2007, 79 Sayfa

Zemin ve yapı arasındaki atalet etkileşimi, temellerin esnekliği sebebiyle yapının dinamik tepki özelliklerinde değişime sebep olabilir. Yapıyı çevrelen zeminlerin esnekliği ve enerji sönümleme yeteneği, yapı salınımlarının peryodunun uzamasına ve sönümlemesinin belirgin şekilde artmasına sebep olabilir. Atalet etkileşimi analizleri, literatürde değişik zemin koşulları ve temel tipleri için verilen frekans-bağımlı temel empadans katsayıları kullanılarak gerçekleştirilebilir. Ancak, bu tip analizlerin frekans uzayında gerçekleştirilmeleri gerektiğinden, sadece lineer yapısal davranış söz konusu olduğunda kullanılabilirler. Diğer taraftan, sabit bir uyarım frekansı kabul edilerek, eşdeğer frekans-bağımsız temel direnç katsayıları hesaplanabilir.

Bu çalışmada, ampirik denklemler veya mod analizi ile elde edilebilecek sabit temel üzerindeki yapının doğal frekansının, empedans formüllerindeki uyarım

frekansı teriminin yerine konabileceği kabul edilmiştir. Ortaya çıkan hesap hatası, frekans-bağımlı ve frekans-bağımsız temel direnç katsayıları kullanılarak incelenmiştir. Analizlerde, tek serbestisi olan lineer salıngaç yapı tepkisinin modellenmesi için kullanılmıştır. Elastik yarı-uzay üzerinde yer alan rijit disk temelin frekans-bağlı direnci az sayıdaki ayrık elemanlar ile modellenmiştir. Hesaplar 72 ivme kaydı kullanılarak frekans uzayında gerçekleştirilmiştir.

Sonuç olarak, atalet etkileşimi etkilerinin orta derecede olduğu durumlarda, sabit temel üzerindeki yapının doğal frekansının etkin uyarım frekansı olarak kullanılabileceği sonucuna varılmıştır. Yapı tepkisi için eşdeğer-lineer yaklaştırması kullanılarak, bu sonucun doğrusal olmayan yapı davranışının incelendiği durumlar için de geçerli olduğu görülmüştür. Ancak, atalet etkileşiminin yapı tepkisi üzerindeki etkisinin daha aşırı olduğu durumlarda, esnek temel üzerinde yer alan yapının doğal frekansının hesapta kullanılmasının daha uygun olacağı görülmüştür. Bu frekans değerinin hesabı, temel direnç katsayılarına bağlı olması sebebi ile, iteratif bir yaklaşım gerektirir.

Keywords: Zemin-yapı etkileşimi, atalet etkileşimi, temel empedansı

To My Beloved Parents,

ACKNOWLEDGEMENTS

I would like to express my gratitude to my supervisor Assoc. Prof. Dr. Bahadır Sadık Bakır for inspiring me to work in the geotechnical field and providing me the oppurtunity to study on this thesis subject.

I am grateful to my co-supervisor Asst. Prof. Dr. Mustafa Tolga Yılmaz for his invaluable guidance, encouragements, insight, advice, criticisms and never-ending support. Without his presence this thesis study would never be thorough.

My special thanks go to Murat Önal, whose benevolent explanations and advice on my computer code helped me construct the basis for my study. I highly appreciate his efforts that assisted me at essential times.

I would like to thank to Metehan Erdoğan, Sevgi Saraç, Ali Şengöz, Yeşim Sema Ünsever and Ümit Taner Yüksekol for their technical and social support throughout my graduate study. Their friendship and professional collaboration means a great deal to me.

I am deeply indebted to my sister, Özge Yılmazok, for her endurance in all the trouble I put her through during my most stressful moments. I am touched by her patience and gentleness.

It was always my parents who believed in me and encouraged me in whatever I do. Their unconditional love and affection I will cherish forever.

TABLE OF CONTENTS

LIST OF TABLES

LIST OF FIGURES

LIST OF ABBREVIATIONS AND SYMBOLS

a_0	Dimensionless frequency
$c(a_0)$	Dimensionless dynamic damping coefficient
$c_h(a_0)$	Dimensionless dynamic damping coefficient for translation
$c_r(a_0)$	Dimensionless dynamic damping coefficient for rocking
c_s	Shear wave velocity of soil
d	Distance
h	Effective height of structure
$\bar{h}$	Slenderness ratio
$\tilde{h}$	Effective height of structure
k	Stiffness
$k(a_0)$	Dimensionless dynamic stiffness coefficient
$k_h(a_0)$	Dimensionless dynamic stiffness coefficient for translation
$k_r(a_0)$	Dimensionless dynamic stiffness coefficient for rocking
m	Mass
$\bar{m}$	Mass ratio
$\tilde{m}$	Effective mass of structure
$\bar{s}$	Stiffness ratio
r_0	Characteristic radius of foundation
u	Structural distortion
u_0 , u_1	Displacements of masses M_0, M_1 of MTM
u_g	Horizontal support excitation (free-field ground motion)
u_h	Lateral displacement of foundation
C_0, C_1	Coefficients for dashpot elements of MTM
G	Shear modulus

K	Static stiffness of foundation
K_h	Static stiffness coefficient for horizontal motion
K_r	Static stiffness coefficient for rocking motion
K_y	Horizontal translation impedance of foundation
K_θ	Rocking impedance of foundation
M	Magnitude of earthquakes
M_L	Richter local magnitude
M_w	Moment magnitude
M_0, M_1	Coefficients for lumped mass elements of MTM
N_{st}	Number of storeys
P_0	Applied load on the system
S_0	Dynamic stiffness of foundation
S_h	Dynamic stiffness factor for horizontal motion
S_r	Dynamic stiffness factor for rotational motion
S_v	Dynamic stiffness factor for vertical motion
T	Fundamental structural period
T_n	Natural period
$\tilde{T}$	Natural period of a flexible-base structure
T_e	Effective period of equivalent linear system
χ_0, χ_1	Dimensionless parameters for damping and mass in MTM
μ	Ductility demand on structure
μ_0, μ_1	Dimensionless parameters for damping and mass in MTM
ν	Poisson's ratio
$\theta(\omega)$	Foundation rotation
ρ	Density
ω	Angular frequency

ω_n	Natural frequency
ξ	Viscous damping ratio of structure
ξ_g	Hysteretic damping ratio of soil
ξ_e	Effective damping ratio of equivalent linear system

CHAPTER 1

INTRODUCTION

1.1 General

The effect of foundation deformability on structural response is ignored in most dynamic response analysis of structures. Seismic excitation is defined through employing the free-field acceleration histories as base motion of structures. Hence, in cases that amplitudes of dynamic reaction forces exerted on foundations are not capable of inducing significant foundation deformations, a fixed base is assumed for structures. However, the deformability of foundations on soft soils can result in significant deviation of actual base motion from free-field ground motion. The assessment of dynamic loads acting on a structure that rests on a flexible base is referred as soil-structure interaction (SSI) analysis.

The basic approach for SSI analysis is known as the direct method, in which the computational model involves both structure and soil. The transient equilibrium equations are solved simultaneously for both structure and continuum elements that model surrounding soil. In order to model unbounded continuum, consistent boundary conditions should be employed for boundaries, such that they should be able to dissipate energy of incident waves. Although the direct method is analytically straightforward, it is computationally expensive and not feasible for parametric studies. An alternative is to employ the substructuring (or, multistep) method, in which continuum and structure are separately analysed in frequency domain, and coupling of both systems is achieved through equilibrium and compatibility equations expressed for the foundation-soil interface by utilising the

superposition principle. Although the substructuring method is computationally more feasible than the direct method, it is applicable only for linear systems.

An important outcome of the substructuring method is that there are basically two different modes of dynamic interaction between soil and foundation: inertial interaction and kinematic interaction (Wolf, 1985). The kinematic interaction results in the modulation of base motion due to impedance contrast between soil and foundation, and it is particularly important for stiff foundations embedded in soft soils. The inertial interaction alters dynamic response characteristics of a structure due to foundation deformability, such that the flexibility and energy dissipation capability of surrounding soil may lead to an increase in period and damping of structural oscillations. The kinematic interaction analysis is sophisticated, and the computational effort is close to the effort necessary for a complete SSI analysis. Nonetheless, through utilisation of frequency dependent foundation impedance coefficients that are reported in literature for various soil conditions and foundation types; the inertial interaction analysis is straightforward (Pecker and Pender, 2000). That is why codes or provisions on aseismic design of structures, such as NEHRP (2003), are able to provide practical approaches for the consideration of inertial interaction in seismic response calculations.

A simple and approximate approach to inertial interaction analysis is to calculate frequency-independent impedance coefficients, through substitution of an effective frequency term for variable excitation frequency terms in impedance expressions. As an example, NEHRP states the use of spring elements with coefficients K_y for horizontal translation impedance and K_θ for rocking impedance of foundation, in order to estimate the fundamental period of a flexible-base structure ($\tilde{T}$) by the equation

$$\tilde{T} = T\sqrt{1+\left(\frac{2\pi}{T}\right)^2 \cdot \frac{\tilde{m}}{K_y} \cdot \left(1+\frac{K_y \tilde{h}^2}{K_\theta}\right)} \tag{1.1}$$

where T is the fundamental structural period when a fixed-base is assumed, $\tilde{m}$ is the effective mass of the structure, and $\tilde{h}$ is the effective height of the structure. Although K_y is relatively insensitive to excitation frequency, frequency-dependency of K_θ can not be ignored. A correction factor for K_θ is proposed as a function of dimensionless parameter $r_0 / c_s T$, where r_0 is the characteristic radius of foundation, and c_s is the shear wave velocity of soil. Theoretically, the frequency $2\pi/\tilde{T}$ is considered as effective frequency. For simplicity, the correction factor is given as a function of T, after manipulation of the theoretical correction factor according to practical ranges of SSI parameters.

This study focuses on the accuracy and precision of approximate inertial interaction analyses in which the fundamental period of a fixed-base structure (T) is used directly for calculation of frequency-independent foundation impedance coefficients. A simple model that is composed of discrete elements is used for simulation of frequency-dependent impedance of a rigid disk foundation resting on homogeneous elastic halfspace. Frequency independent impedance coefficients are determined through substitution of the natural frequency of fixed-base structure (ω_n), which is modelled as a single-degree-of-freedom (SDOF) oscillator, for the excitation frequency terms in foundation impedance expressions. Furthermore, the impact of frequency-dependency of foundation impedance for nonlinear structural response is evaluated by equivalent linearization.

1.2 Literature Review

The primary effect of inertial interaction on structural response is to elongate the period and to increase damping of the oscillations. The significance of inertial interaction on structural response can be examined through investigation of the ratio $\tilde{T}/T$, as well as through comparisons of fixed base and flexible base damping characteristics of a structure. The simplest approach is to introduce flexible supports for a SDOF oscillator that is representative for the fundamental mode of fixed-based structure. The approach can lead to simple formulae for estimation of fundamental period and damping ratio of a flexible-base structure, such as those provided by Veletsos and Meek (1974) considering a rigid disk foundation on elastic halfspace. For the case of a cylindrical foundation embedded into viscoelastic soil layer over rigid bedrock, Avilés and Pérez-Rocha (1999) presented diagrams for fundamental period and damping of flexible-base structures. Later, Avilés and Suárez (2002) extended the study for the cases of soil over elastic bedrock.

These studies confirmed that the ratio $\tilde{T}/T$ is most sensitive to the dimensionless parameter r_0/c_sT. Comparison of foundation impedances for embedded and surficial foundations reveals that the ratio $\tilde{T}/T$ is larger for a surficial foundation, whereas the damping ratio of a flexible-base structure is larger for an embedded foundation (Veletsos and Nair, 1975). The importance of dimensionless parameter r_0/c_sT for nonlinear structural response was shown by Avilés and Pérez-Rocha (2005). Furthermore, the damping due to hysteretic response of soils is almost as important as the damping due to radiation of waves to unbounded domain (Ambrosini, 2006).

Most of the seismic design codes provide idealized smooth acceleration spectra which attain a constant spectral acceleration plateau in the short period range, and show a monotonic decrease in the mid-period range. This allows the assumption that the inertial interaction has beneficial effect on structural performance, and fixed-base response of structures can be conservatively introduced in design calculations. Employing dynamic response analyses, Ciampoli and Pinto (1995), and later Elnashai and McClure (1996) showed that the ignorance of inertial interaction for nonlinear structural response computations is acceptable. However, particular cases that inertial interaction can be detrimental for structures are discussed in literature.

When soft site records are employed, the increase in period can raise inelastic displacement demand on a structure for certain structural period ranges (Miranda and Bertero, 1994). The effect of inertial interaction on structural response becomes detrimental as the natural frequency of oscillations approaches to the dominant frequency of ground shaking, but it is beneficial for structures with fundamental period longer than the site period (Avilés and Pérez-Rocha, 1998, 2003; Şafak, 2006; Mylonakis and Gazetas, 2000). SSI can also result in a decrease in strength reduction coefficients, leading to an unconservative design when SSI is ignored in seismic load calculations for structures on soft soils (Ghannad, and Jahankhah, 2007). Therefore, in order to prevent an unsafe design, clause 6(1) of EN1998-5 (CEN, 2004) imposes the consideration of SSI in seismic design of slender tall structures, and in seismic design of structures on very soft soils.

For the case of rigid foundation on elastic halfspace, the foundation impedance to dynamic excitation in each direction can be described by a spring and a dashpot element connected to central node of foundation. The spring and dashpot coefficients are dependent on the excitation frequency, and obtained through numerical or analytical approaches for calculation of dynamic response of elastic

continuum. Veletsos and Wei (1971), and later Veletsos and Verbic (1973, 1974) provided rigorous solutions for a disk foundation resting on elastic or viscoelastic halfspace. A set of formulae for frequency-dependent impedance coefficients of arbitrarily-shaped shallow foundations, which were verified by model tests, is available in literature for practical engineering applications (Dobry and Gazetas, 1986; Gazetas, 1991). For the cases that the computation of frequency-dependent impedance coefficients for a particular foundation type and soil profile is necessary, computationally less expensive techniques, such as the use of cone model (Takewaki et al, 2003) or as the use of uniformly distributed spring elements beneath the foundation (Nogami et al, 2001), are available. However, the frequency-dependency of foundation impedance coefficients invokes the necessity for performing the SSI analyses in frequency domain.

When nonlinear structural response should be considered, it is possible to perform inertial interaction analyses in time domain through defining a representative frequency (or, period) of excitation for calculation of frequency-independent foundation impedance coefficients. As an example, NEHRP (2003) recommends the use of the natural period of the structure on flexible base (i.e., $\tilde{T}$), or the natural period of the fixed-base structure with minor modifications on impedance coefficients, in order to estimate representative frequency of excitation. However, when frequency-independent impedance coefficients are employed, the nonlinear response of structure can be sensitive to the selection of the representative frequency (Ghannad and Jahankhah, 2007). The alternative and more rigorous approach is to use simple models that are composed of discrete elements with frequency-independent coefficients, such that these models are capable of simulating the response of elastic continuum with sufficient accuracy.

Simple discrete models with a limited number of mass, dashpot, and spring elements that have frequency-independent coefficients can simulate the response of

elastic halfspace in time-domain analyses (Wolf and Somaini, 1986). The model, namely the *Monkey-Tail Model*, was found to be in good agreement with rigorous solutions for a rigid disk on elastic halfspace (Wolf, 1997). Alternative simple models were developed by the use of serially connected oscillators (Wu and Chen, 2001), or by the use of gyromass element which generates inertial reaction force proportional to the relative acceleration between selected nodes (Saitoh, 2007).

1.3 Objective and Scope

The objective of this study is to provide an assessment of the accuracy and precision of approximate inertial interaction analyses in which frequency-independent foundation impedance coefficients are employed. Particularly, it is supposed that the fundamental frequency of the fixed-based structure is used for calculation of frequency-independent impedance coefficients. The analyses are performed for a set of dimensionless parameters that are representative for most structures resting on soils. The acceleration histories used for dynamic response analyses were recorded on soil sites and were pertinent to 36 different events. Both horizontal components of a recorded motion are employed. No special emphasis on directivity and topographic amplification effects is put. The study aims to provide possible error ranges for structural displacement calculations that are induced by ignorance of frequency-dependency of impedance functions. The study does not provide any statistical discussions on results, since a rigorous sampling procedure for earthquake records is necessary for reliable statistical conclusions.

The response of a single degree of freedom oscillator is supposed to be representative for structural response. The damping ratio for elastic response of structure is chosen as 5%. The foundation is considered as a rigid disk resting on homogeneous elastic halfspace. No foundation embedment is considered, since the

longest natural period elongation due to inertial interaction is obtained for a surficial foundation.

The *Monkey-Tail Model* is employed in order to simulate the frequency-dependent impedance of a rigid disk on elastic halfspace. However, in order to calculate frequency-independent impedance coefficients, it is assumed that the excitation frequency is equal to the fundamental frequency of fixed-base structure. The improvement on results of approximate inertial interaction analyses through the use of fundamental frequency of flexible-base structure is also assessed. All dynamic response analyses are performed in frequency domain. The dimensionless SSI parameters that significantly increase the magnitude of approximation error are discussed. Besides, two records that cause low and large variability in results are criticized.

Finally, the study extends the application of methodology to cases of nonlinear structural response through employing equivalent linearization. Two levels of nonlinear response are taken into consideration through setting 4 and 7 as the ductility demand (μ) on structure. The effective period and damping ratio of the structure is estimated through equivalent linearization relationships. On the other hand, the fundamental period pertinent to linear response is utilised for the calculation of frequency-independent impedance coefficients. The difference between maximum structural distortions computed through employing frequency-dependent and frequency-independent impedance coefficients is evaluated.

This thesis is composed of four chapters. The object and scope of the study, and a brief literature review is given in the first chapter.

Chapter 2 presents the computational procedure, the range of parameters employed in analyses, and the computer programs developed for the study. Besides, summary information on the earthquake records is given.

Chapter 3 presents the results of parametric analyses. For a given set of dimensionless parameters, analyses are performed for 72 acceleration histories and for a practical range of structural period. The significance of dimensionless parameters as well as the error induced in computation of maximum structural distortion by frequency-independent impedance coefficients is evaluated.

Finally, a summary of the study and the conclusions are given in Chapter 4.

CHAPTER 2

METHODOLOGY

2.1 The Lumped Parameter Model

The *Monkey-Tail Model* (MTM) is adapted to model the dynamic impedance of shallow foundations without embedment (Wolf, 1997). Implementation of MTM is simple and provides sufficient accuracy in calculation of dynamic foundation impedance. MTM involves one spring element with coefficient K representing the static stiffness of the foundation, one dashpot element with coefficient C_0, and two lumped mass elements with coefficients M_0 and M_1 linked to two degrees of freedom u_0 and u_1 respectively (Figure 2.1). u_0 is the displacement of the centre of the massless rigid disk foundation under load P_0. u_1 is the displacement of mass M_1, and has no physical meaning, but is necessary for approximation of the frequency-dependent foundation impedance. One MTM is implemented separately for each degree of freedom of the rigid disk foundation. Formulation of frequency-dependent dynamic stiffness coefficients for horizontal translation ($S_h(\omega)$), vertical translation ($S_v(\omega)$), and rocking ($S_r(\omega)$) modes of foundation vibration is straightforward.

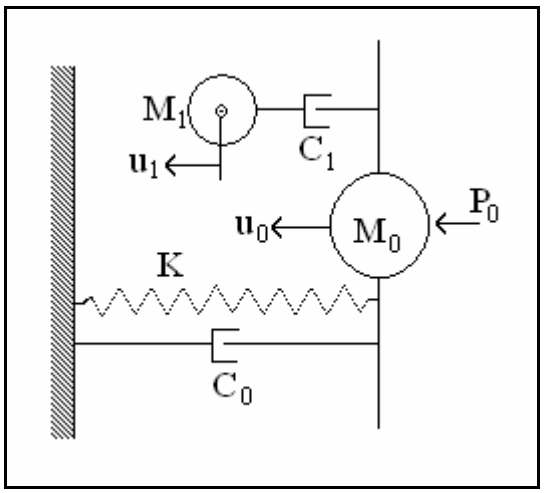

Figure 2.1 – The Monkey-Tail Model

For a disk foundation resting on homogeneous elastic halfspace, the parameters C_0, C_1, M_0 and M_1 are specified as

$$C_0 = \frac{r_0}{c_s}\chi_0 K \tag{2.1.a}$$

$$C_1 = \frac{r_0}{c_s}\chi_1 K \tag{2.1.b}$$

$$M_0 = \frac{r_0^{\,2}}{c_s^{\,2}}\mu_0 K \tag{2.1.c}$$

$$M_1 = \frac{r_0^{\,2}}{c_s^{\,2}}\mu_1 K \tag{2.1.d}$$

where r_0 is the radius of the foundation, c_s is the shear wave velocity of the elastic halfspace, and $\chi_0, \chi_1, \mu_0, \mu_1$ are dimensionless parameters. The relationship between shear wave velocity c_s, density ρ, and shear modulus G for an elastic medium is

$$c_s = \sqrt{G/\rho} \tag{2.2}$$

The static stiffness K and the dimensionless parameters $\chi_0, \chi_1, \mu_0, \mu_1$ are functions of G, r_0 and the Poisson's ratio ν of halfspace (Table 2.1).

Table 2.1 - Static stiffness and dimensionless coefficients of MTM for rigid disk on homogeneous halfspace (Wolf, 1997)

	Static Stiffness	**Dimesionless Coefficients**			
	K	χ_0	χ_1	μ_0	μ_1
Horizontal	$\frac{8 G r_0}{2-\nu}$	$0.78 - 0.4\nu$	——	——	——
Rocking	$\frac{8 G r_0^3}{3(1-\nu)}$	——	$0.42 - 0.3\nu^2$	$\nu < 1/3 \quad 0$ $\nu > 1/3 \quad 0.16(\nu - 1/3)$	$0.34 - 0.2\nu^2$

For harmonic excitation of frequency ω, the dynamic stiffness of the foundation is defined as:

$$S_0(a_0) = P_0(a_0)/u_0(a_0) \tag{2.3}$$

where, a_0 is the dimensionless frequency defined as

$$a_0 = \omega r_0 / c_s \tag{2.4}$$

Thus, in frequency domain, the dynamic stiffness of the foundation for each degree of freedom involves a real and an imaginary part, which can be normalised by the static spring stiffness as given in the following:

$$S_0(a_0) = K\left[k(a_0) + i\, a_0\, c(a_0)\right] \tag{2.5}$$

where $k(a_0)$ and $c(a_0)$ are the dimensionless dynamic stiffness and damping coefficients, which are obtained through derivation of equilibrium equations for the MTM and substitution of equations 2.1 into equilibrium equations (Wolf, 1994):

$$k(a_0) = 1 - \frac{\mu_1 a_0^2}{1 + \frac{\mu_1^2}{\chi_1^2} a_0^2} - \mu_0 a_0^2 \tag{2.6.a}$$

$$c(a_0) = \frac{\mu_1}{\chi_1} \cdot \frac{\mu_1 a_0^2}{1 + \frac{\mu_1^2}{\chi_1^2} a_0^2} + \chi_0 \tag{2.6.b}$$

The dimensionless stiffness and damping coefficients can be calculated by employing Table 2.1. A good agreement between the dimensionless stiffness and damping coefficients according to MTM and rigorous analytical solutions exists (Wolf, 1994, 1997). The comparisons for rocking impedance of rigid disk foundation resting on elastic halfspace are presented in Figure 2.2.

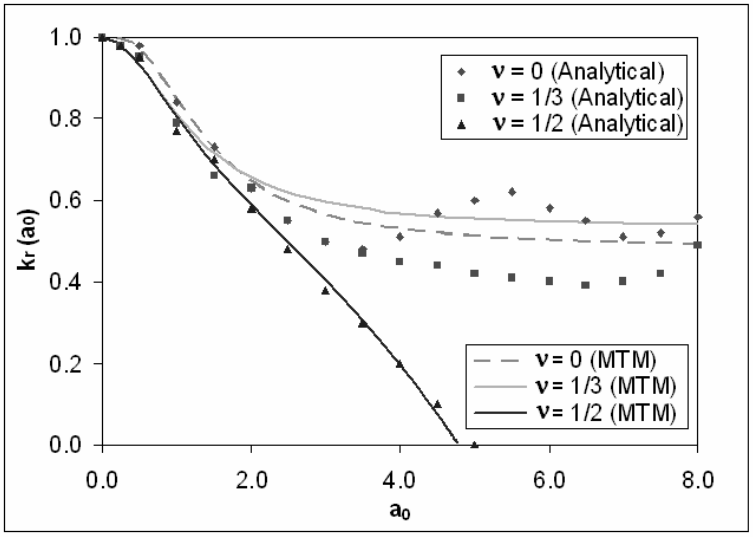

(a)

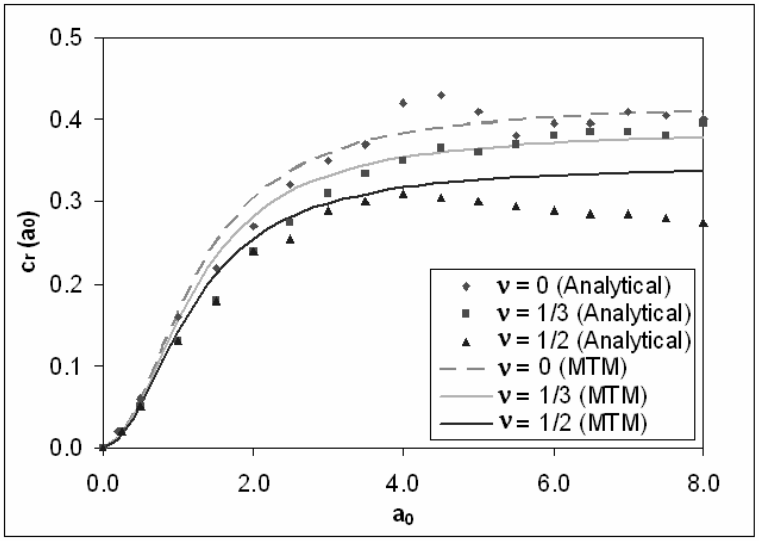

(b)

Figure 2.2 – Comparisons of dimensionless rocking (a) stiffness and (b) damping coefficients according to MTM with those according to analytical solutions provided by Veletsos and Wei (1971). The figure is reproduced after Wolf (1994).

2.2 The Equations of Motion for Simple Interaction Analysis

The structure is idealized with a concentrated mass m, spring with stiffness k, dashpot with viscous damping coefficient c that are connected horizontally to a massless rigid bar of length h (Figure 2.3). The natural frequency of the fixed-base structure is

$$\omega_n = \sqrt{\frac{k}{m}} \tag{2.7}$$

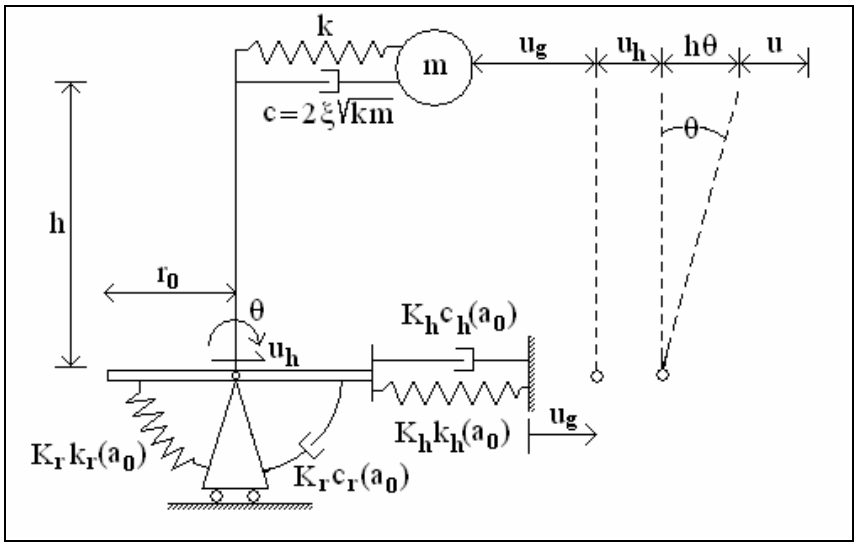

Figure 2.3 – The structure model with horizontal and rocking motions applied on

Hence, the period of the structure, T_n, is equal to $2\pi/\omega_n$. Omitting the vertical excitation, the simple soil-structure interaction model has three degrees of freedom. Those are the lateral displacement of the foundation $u_h(\omega)$, the foundation rotation $\theta(\omega)$, and the transverse displacement of the beam $u(\omega)$ representing the structural distortion. The equilibrium of the interaction model in Figure 2.3 under

horizontal support excitation $u_g(\omega)$ leads to three equations in frequency domain (Wolf, 1994):

$$\begin{bmatrix} \omega_n^2(1+2i\xi\frac{\omega}{\omega_n})-\omega^2 & -\omega^2 & -\omega^2 \\ -\omega^2 & \frac{S_h(a_0)}{m}-\omega^2 & -\omega^2 \\ -\omega^2 & -\omega^2 & \frac{S_r(a_0)}{mh^2}-\omega^2 \end{bmatrix} \begin{Bmatrix} u(\omega) \\ u_h(\omega) \\ h\theta(\omega) \end{Bmatrix} = -\begin{Bmatrix} 1 \\ 1 \\ 1 \end{Bmatrix} \ddot{u}_g(\omega) \qquad (2.8)$$

The reason for consideration of viscous damping for modelling the energy dissipation characteristic of structure is to provide compatible results with time-domain response analyses reported in literature. Nonetheless, the analyses are performed in frequency domain, through employing Fast Fourier Transform (FFT) algorithm.

2.3 Calculation of Foundation Impedance Coefficients

The significance of soil-structure interaction is related to the properties of the soil and the structure. The following dimensionless parameters are sufficient to define the dynamic response characteristics of the simple soil-structure interaction model in Figure 2.3 (Wolf, 1994):

- The stiffness ratio, $\bar{s}$;

$$\bar{s} = \frac{\omega_n h}{c_s} \qquad (2.9.a)$$

- The slenderness ratio, $\bar{h}$;

$$\bar{h} = \frac{h}{r_0} \qquad (2.9.b)$$

- The mass ratio, $\overline{m}$

$$\overline{m} = \frac{m}{r_0^3 \rho} \tag{2.9.c}$$

- The damping ratios of soil, ξ_g, and structure ξ
- The Poisson's ratio of soil, ν

Employing equation 2.5, the frequency dependent horizontal and rocking impedance coefficients, $S_h(a_0)$ and $S_r(a_0)$ respectively, are computed by

$$S_h(a_0) = K_h\left[k_h(a_0) + i\, a_0\, c_h(a_0)\right] \tag{2.10.a}$$

$$S_r(a_0) = K_r\left[k_r(a_0) + i\, a_0\, c_r(a_0)\right] \tag{2.10.b}$$

The static stiffness coefficients on the right side of the equalities in 2.10 are expressed in terms of the dimensionless parameters $\overline{s}$, $\overline{h}$ and $\overline{m}$, as given in the following:

$$K_h = \frac{8\,\omega_n^2}{2-\nu} \cdot \frac{m\,\overline{h}^2}{\overline{m}\,\overline{s}^2} \tag{2.11.a}$$

$$K_r = \frac{8\,\omega_n^2}{3(1-\nu)} \cdot \frac{m\,h^2}{\overline{m}\,\overline{s}^2} \tag{2.11.b}$$

When hysteretic damping of soil should be considered in analyses, the static stiffness coefficients should be multiplied by the factor $1+2i\xi_g$ in frequency domain, according to the correspondence principle (Wolf, 1985). Besides, the dimensionless frequency is expressed in terms of the dimensionless parameters, through substitution of equations 2.9.a and 2.9.b into equation 2.4,

$$a_0 = \frac{\bar{s} \cdot \omega}{\bar{h} \cdot \omega_n} \tag{2.12}$$

Finally, the dimensionless dynamic stiffness and damping coefficients are reduced to following simpler forms through employing Table 2.1 and equations 2.6.a and 2.6.b:

$$k_h(a_0) = 1 \tag{2.13.a}$$

$$c_h(a_0) = \chi_0 \tag{2.13.b}$$

$$k_r(a_0) = 1 - \frac{\mu_1 a_0^2}{1 + \frac{\mu_1^2}{\chi_1^2} a_0^2} \tag{2.13.c}$$

$$c_r(a_0) = \frac{\mu_1}{\chi_1} \cdot \frac{\mu_1 a_0^2}{1 + \frac{\mu_1^2}{\chi_1^2} a_0^2} \tag{2.13.d}$$

2.4 Procedure

Considering a range of dimensionless soil-structure interaction parameters, and a range of structural period, the maximum structural distortion (u) is computed through employing equation 2.8 with 72 earthquake records. The dynamic response is computed in frequency domain, considering that

- foundation impedance is dependent on the excitation frequency, such that dimensionless impedance coefficients $k(a_0)$ and $c(a_0)$ are computed for each excitation frequency, and
- foundation impedance is frequency-independent, such that dimensionless impedance coefficients $k(a_0)$ and $c(a_0)$ are computed by employing a constant dimensionless frequency instead of the excitation frequency.

For the latter case, it is assumed that the natural frequency of the fixed-based structure (ω_n) is the optimum choice for a constant dimensionless frequency. Thus, the equality $\omega = \omega_n$ is substituted in equation 2.12 for calculation of coefficients $k(a_0)$ and $c(a_0)$. In order to investigate the significance of frequency-dependency of foundation impedance for peak structural distortion, the ratio of maximum absolute structural distortions due to two procedures is calculated for each record. Finally, since actual response of a typical building under severe seismic excitation is nonlinear, the effect of nonlinear structural response on the previously obtained results is investigated through employing an equivalent linear model for the structure. The details of the analyses are presented in the following.

2.4.1 The Computer Program

A computer program, which computes dynamic response of the simple interaction model through employing Fast Fourier Transform (FFT) algorithm, is developed in Matlab computing environment. The program comprises one main analysis program, "AnalysisMain," that calls four routines, "MTMMultiple," "MTMSingle," "Multiple," and "Single". The codes are listed in Appendix A.

The main program, "AnalysisMain", calls the routines "MTMMultiple" and "MTMSingle" with input parameters ω_n, ν, ξ, $\bar{s}$, and $\bar{h}$. Then, the main program calculates the ratio of maximum absolute structural distortions, namely the displacement ratio, computed by these routines for each earthquake record, calculates the mean and standard deviation of computed data, and plots the results. The computational procedure is repeated for each period step.

The "MTMMultiple" routine calls the routine "Multiple" for each acceleration history and stores the absolute value of computed displacements.

The "Multiple" routine calculates response of the simple soil-structure interaction system to a given horizontal base excitation. Hence, the system of equations 2.8 is solved in frequency domain. The static stiffnesses K_h and K_r are calculated employing the dimensionless parameters $\bar{s}$, $\bar{h}$ and ω_n (equations 2.11). The frequency-dependent foundation impedance parameters, $k(a_0)$ and $c(a_0)$ are calculated for each excitation frequency below the Nyquist frequency. The time-history of structural distortion (u) is computed by the inverse Fourier transform, and is returned to the routine "MTMMultiple".

The "MTMSingle" routine is similar to "MTMMultiple" and calls the routine "Single" instead of the routine "Multiple".

Similar to the routine "Multiple", the routine "Single" computes the time-history of structural distortion for the set of earthquake records. However, instead of computing frequency-dependent impedance coefficients $k(a_0)$ and $c(a_0)$ separately for each excitation frequency, these coefficients are kept constant for all frequencies, such that the equality $\omega = \omega_n$ is substituted into equation 2.12 for calculation of a_0. The other calculation steps show no difference from those of the routine "Multiple".

2.4.2 Selection of the Non-dimensional Parameters

The ranges of dimensionless parameters, $\bar{s}, \bar{h}, \text{and } \bar{m}$, are chosen according to practical applications. Actually, the parameters $\bar{m}$ and $\bar{h}$ are correlated to each other since both height and mass of a structure are proportional to the number of

storeys of a building, N_{st}. Supposing that mass per unit area on each storey is 1 ton/m^2, the mass of a multi-storey structure is approximately

$$m = 1^{\text{ton/m}^2} \cdot N_{st} \cdot \pi r_0^2 \tag{2.14}$$

where, πr_0^2 is equal to the area of each storey. Assuming that the storey height is 3^m, that the mass of the building is lumped at two-thirds of building height, and that the density of soil (ρ) is 1.6 t/m^3, it is straightforward to show that

$$\overline{m} \cong \overline{h} \tag{2.15}$$

Thus, the dimensionless parameters $\overline{m}$, and $\overline{h}$ are proportional and approximately equal for practical applications. Since an arbitrary selection of dimensionless parameters may be pertinent to an unrealistic soil-structure interaction problem, equation 2.15 is employed in order to estimate $\overline{m}$ for a selected value of $\overline{h}$. Hence, the dimensionless parameters $\overline{s}$, $\overline{m}$, and $\overline{h}$ are approximated as 1 for a typical 5-storey reinforced concrete building on soft soil. The selected range of $\overline{s}$ and $\overline{h}$ is between 0.5 and 2.0 in the analyses, so that the effect of inertial interaction on structural response is moderate. Except for the analyses investigating the significance of hysteretic damping ($\xi_{g)}$ and Poisson's ratio (ν) of soil in results, ν is set to 0.3, which is representative for drained soil behaviour, and ξ_g is set to zero. The structural damping ratio, ξ, is set as 5%. The analyses are performed for fixed-base structural periods between 0.2 and 2.0 seconds.

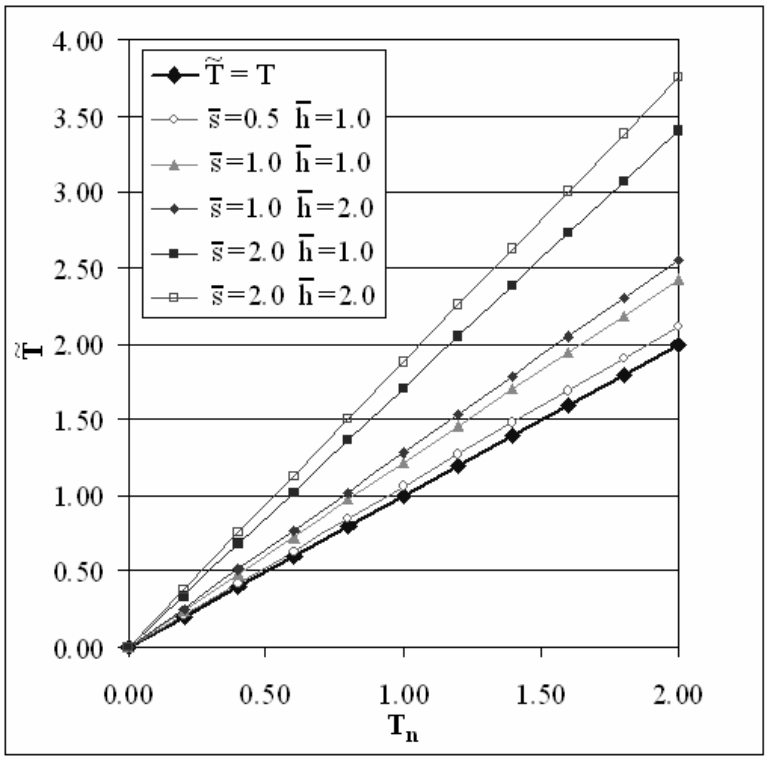

Figure 2.4 – Comparison of natural period with the flexible-base period $\tilde{T}$

Utilizing equation 1.1, the comparison of the natural period of the fixed-base SDOF oscillator with that of the flexible-base oscillator is presented in Figure 2.4, for the ranges of dimensionless parameters utilised in the analyses. The case with $\bar{s} = 2$ and $\bar{h} = 2$ indicates the longest period elongation due to inertial interaction for the selected range of parameters. When $\bar{s}$ is less than 2, it is accepted that the effect of inertial interaction on structural response is moderate.

2.4.3 Equivalent Linear Model for Nonlinear Structural Response

The nonlinear response of structures to severe seismic excitation may effect the significance of frequency-dependency of foundation impedance for peak structural

distortion. Since the analysis procedure is applicable only for linear systems, nonlinear structural response is approximated by an equivalent linear model. According to Iwan (1980), a good approximation of response of a bilinear single degree of freedom oscillator is obtained with a linear system with period

$$T_e = \left[1 + 0.121(\mu - 1)^{0.939}\right] \cdot T_n \tag{2.16}$$

and damping,

$$\xi_e = \xi + 0.0587(\mu - 1)^{0.371} \tag{2.17}$$

where T_n and ξ are the natural period and damping ratio of the elastic response, and μ is the ductility demand on the inelastic response.

The analyses that consider inelastic response of the structure are conducted through employing $2\pi / T_e$ and ξ_e instead of ω_n and ξ in equation 2.8. However, the dimensionless frequency a_0 is calculated by using T_n in analyses with frequency-independent foundation impedance coefficients, since it is straightforward to compute natural period of structure, prior to transient analysis. $\bar{s}$ is equal to 2.0 for analyses that consider the nonlinear response of structure, so that impact of soil-structure interaction on structural response is more significant. Besides, in order to consider different levels of structural nonlinearity, μ is set to 4 and 7 for two different sets of analyses. The results for nonlinear structural response are compared with those for linear structural response.

2.5 Earthquake Records

A total of 72 acceleration records, which involves 36 different events and consist of two horizontal components of motions, is utilised for the analyses. The records have been downloaded from two different sources: COSMOS Virtual Data Center (COSMOS, 2004) and PEER Strong Motion Database (PEER, 2006). For the selection of records from the databases, the lowest peak ground acceleration is chosen as 0.092g. The range of earthquake magnitudes is $4.9 \leq M \leq 8.0$, given as moment magnitude (M_w) except for the Taiwan Smart1 (5) 01/29/81 record which is given as Richter local magnitude (M_L). The source distances of records are based either on the shortest distance to the fault rupture or as hypocentral distance (Kramer, 1996), and cover the range 6.0 km $\leq d \leq$ 116.8 km. The distribution of earthquake records according to magnitude and distance is presented in Figure 2.5.

All chosen recording stations were located on soil site. The NEHRP and Geomatrix site classification systems are used for selection of records from the PEER database. The NEHRP site class is based on average shear wave velocity of uppermost 30 m of soil profile (Table 2.2). The Geomatrix Soil Classification system employs three letters in order to classify the conditions for instrument housing, local geology, and geotechnical site conditions. The third letter, which is pertinent to geotechnical subsurface characteristics for the recording site, classifies the sites according the soil thickness and subsurface topography (Table 2.3). The selected records from PEER database belong to sites that correspond to D or E in NEHRP, and C, D and E in Geomatrix classification systems. For consistency, the records from the COSMOS database belong to “alluvium” and “soft soil” classes, since a general description for site conditions are provided for some of the records. No particular emphasis on rupture directivity or subsurface topography effects is put.

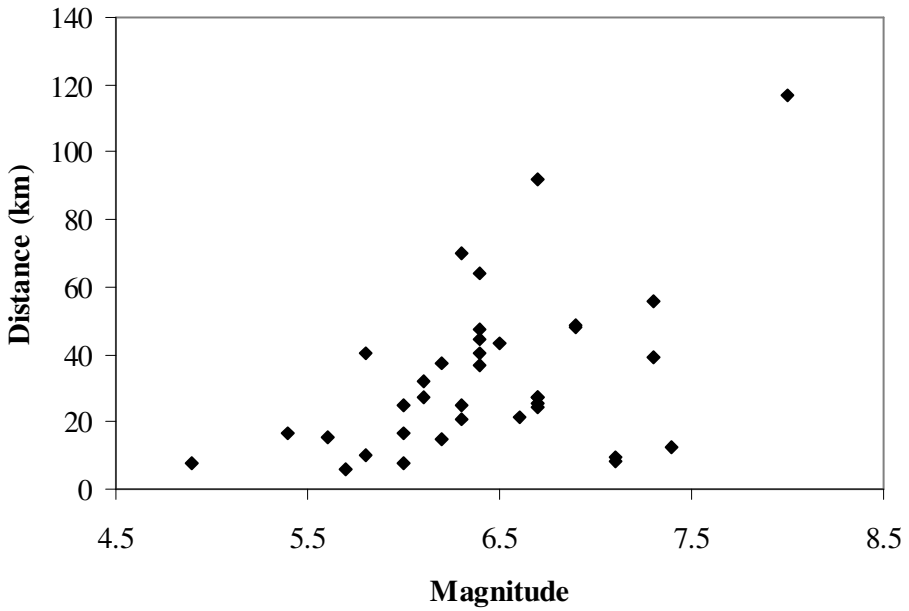

Figure 2.5 – The scatterplot showing the distribution of earthquake magnitude vs. distance for the set of selected records.

Table 2.2 - NEHRP Site Classification, (NEHRP, 2003).

Site Class	Definition	Average c_s of uppermost 30 m of soil profile
A	Hard Rock	≥ 1,500 m/s
B	Rock	760-1,500 m/s
C	Very Dense Soil and Soft Rock	360-760 m/s
D	Stiff Soil	180-360 m/s
E	Soft Soil	≤ 180 m/s

Table 2.3 – Geomatrix 3-Letter Site Classification

Third Letter: Geotechnical Subsurface Characteristics (PEER, 2006)

Site Class	Definition	Condition
A	Rock	Rock (c_s > 600 m/s) or soil up to 5 m thick overlying rock
B	Shallow (stiff) Soil	Soil profile up to 20 m thick overlying rock
C	Deep Narrow Soil	Soil profile at least 20 m thick overlying rock, in a narrow canyon or valley no more than several km wide
D	Deep Broad Soil	Soil profile at least 20 m thick overlying rock, in a broad valley
E	Soft Deep Soil	Deep soil profile with average c_s less than 150 m/s

The control motion employed in the interaction analyses is the free-field motion, and the most convenient records that reflect the free-field motion are the ones that were recorded by an instrument in a shelter at the ground level. However, in order to involve records from a wider range of events, acceleration histories that were recorded on 1-storey buildings are included in the data set, assuming that frequency content of recorded motion involve limited contamination due to the response of housing structure.

The acceleration spectrum of each record is normalised by the average pseudo-spectral acceleration (PSA) in the short period range, $0.1 \leq T \leq 0.5$ (Borcherdt, 1994). The normalised spectra are presented in Figure 2.6. A visual investigation of the normalised spectra and the mean normalised spectrum indicates a common trend by having the peak PSA located within the short period range. Only a few certain earthquakes are observed to have peak PSA located out of this range. Table 2.4 summarizes categorical properties of the employed earthquake records.

In order to study the importance of site condition for record selection, a second set of records that are pertinent to 4 different earthquakes and rock sites is used. The summary information on 8 records is given on Table 2.5. The normalised spectra and the mean normalised spectrum of the second set of records are shown on Figure 2.7. A steep descent in spectral values after the period of 0.2 second is observed for rock spectra, when compared spectra of soil sites.

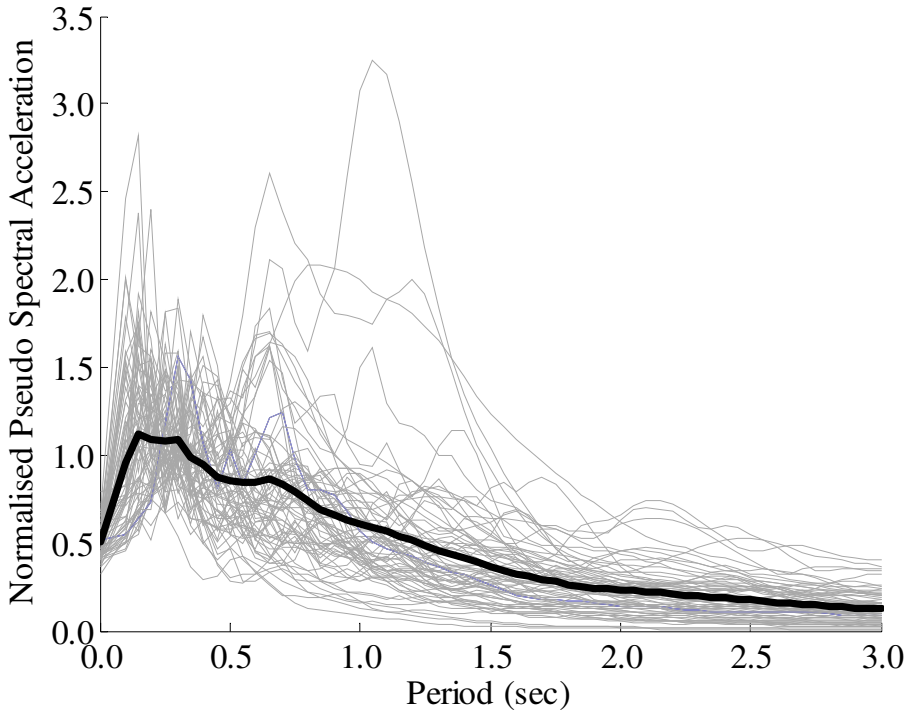

Figure 2.6 – Normalised Earthquake Spectra of Records on Soil Sites.

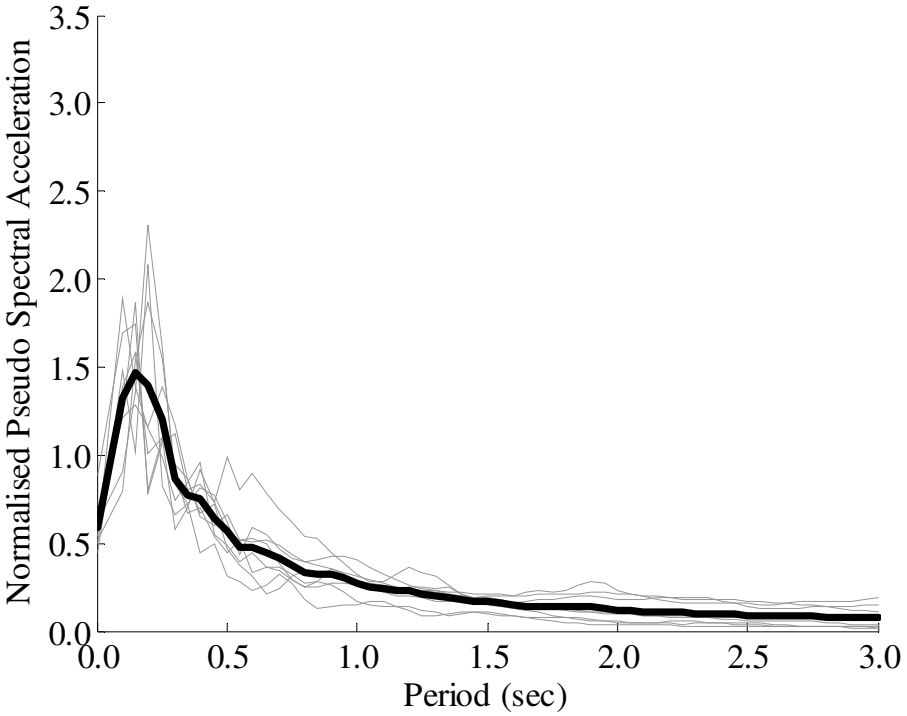

Figure 2.7 – Normalised Earthquake Spectra of Records on Rock Sites.

TABLE 2.4 The List of the selected earthquakes for analyses

Record #	Earthquake	Magnitude (M)	Fault	Station	Component	Site Classification	Distance (d) (km)	PGA (g)	Instrument Housing
	Strong Ground Motion data from PEER								
1	Cape Mendocino, 04/25/92	7.1	thrust/reverse	Petrolia	0	NEHRP-D/ Geomatrix D	9.5 (fault)	0.590	Free Field / Instr. Str.
2	Cape Mendocino, 04/25/92	7.1	thrust/reverse	Petrolia	90	NEHRP-D/ Geomatrix D	9.5 (fault)	0.662	Free Field / Instr. Str.
3	Coalinga, 05/02/83	6.4	thrust/reverse	Parkfield Cholame - 5W	270	NEHRP-D/ Geomatrix C	47.3 (fault)	0.147	Free Field / Instr. Str.
4	Coalinga, 05/02/83	6.4	thrust/reverse	Parkfield Cholame - 5W	360	NEHRP-D/ Geomatrix C	47.3 (fault)	0.131	Free Field / Instr. Str.
5	Coalinga, 05/02/83	6.4	thrust/reverse	Parkfield Fault Zone 1	0	Geomatrix D	40.4 (fault)	0.194	Free Field / Instr. Str.
6	Coalinga, 05/02/83	6.4	thrust/reverse	Parkfield Fault Zone 1	90	Geomatrix D	40.4 (fault)	0.111	Free Field / Instr. Str.
7	Coyote Lake, 08/06/79	5.7	strike-slip	Gilroy Array #3	50	NEHRP-D/ Geomatrix D	6.0 (fault)	0.272	Free Field / Instr. Str.
8	Coyote Lake, 08/06/79	5.7	strike-slip	Gilroy Array #3	140	NEHRP-D/ Geomatrix D	6.0 (fault)	0.228	Free Field / Instr. Str.
9	Hollister, 01/26/86	5.4	strike-slip	Hollister Diff Array #1	255	Geomatrix D	16.9 (hypo)	0.101	Free Field / Instr. Str.
10	Hollister, 01/26/86	5.4	strike-slip	Hollister Diff Array #1	345	Geomatrix D	16.9 (hypo)	0.114	Free Field / Instr. Str.
11	Imperial Valley, 10/15/79	6.5	strike-slip	Delta	262	NEHRP-D/ Geomatrix D	43.6 (fault)	0.238	Free Field / Instr. Str.
12	Imperial Valley, 10/15/79	6.5	strike-slip	Delta	352	NEHRP-D/ Geomatrix D	43.6 (fault)	0.351	Free Field / Instr. Str.
13	Landers, 06/28/92	7.3	strike-slip	Indio - Coachella Canal	0	NEHRP-D/ Geomatrix D	55.7 (fault)	0.104	Free Field / Instr. Str.
14	Landers, 06/28/92	7.3	strike-slip	Indio - Coachella Canal	90	NEHRP-D/ Geomatrix D	55.7 (fault)	0.109	Free Field / Instr. Str.

TABLE 2.4 (Cont'd)

Record #	Earthquake	Magnitude (M)	Fault	Station	Component	Site Classification	Distance (d) (km)	PGA (g)	Instrument Housing
	Strong Ground Motion data from PEER								
15	Loma Prieta, 10/18/89	6.9	oblique	Redwood City	43	NEHRP-E/ Geomatrix D	47.9 (fault)	0.274	Free Field / Instr. Str.
16	Loma Prieta, 10/18/89	6.9	oblique	Redwood City	133	NEHRP-E/ Geomatrix D	47.9 (fault)	0.220	Free Field / Instr. Str.
17	Mammoth Lakes, 05/31/80	4.9	strike-slip	Fish & Game (FIS)	0	Geomatrix D	7.7 (hypo)	0.281	Free Field / Instr. Str.
18	Mammoth Lakes, 05/31/80	4.9	strike-slip	Fish & Game (FIS)	90	Geomatrix D	7.7 (hypo)	0.145	Free Field / Instr. Str.
19	Morgan Hill, 04/24/84	6.2	strike-slip	Gilroy Array #2	0	NEHRP-D/ Geomatrix D	15.1 (fault)	0.162	Free Field / Instr. Str.
20	Morgan Hill, 04/24/84	6.2	strike-slip	Gilroy Array #2	90	NEHRP-D/ Geomatrix D	15.1 (fault)	0.212	Free Field / Instr. Str.
21	Mt. Lewis, 03/31/86	5.6	unknown	Halls Valley	0	NEHRP-D/ Geomatrix C	15.5 (hypo)	0.140	Free Field / Instr. Str.
22	Mt. Lewis, 03/31/86	5.6	unknown	Halls Valley	90	NEHRP-D/ Geomatrix C	15.5 (hypo)	0.159	Free Field / Instr. Str.
23	North Palm Springs, 07/08/86	6.0	reverse-oblique	Palm Springs Airport	0	NEHRP-D/ Geomatrix D	16.6 (fault)	0.158	Free Field / Instr. Str.
24	North Palm Springs, 07/08/86	6.0	reverse-oblique	Palm Springs Airport	90	NEHRP-D/ Geomatrix D	16.6 (fault)	0.187	Free Field / Instr. Str.
25	Northridge, 01/17/94	6.7	thrust/reverse	LA Hollywood Stor FF	90	NEHRP-D/ Geomatrix D	25.5 (fault)	0.231	Free Field / Instr. Str.
26	Northridge, 01/17/94	6.7	thrust/reverse	LA Hollywood Stor FF	360	NEHRP-D/ Geomatrix D	25.5 (fault)	0.358	Free Field / Instr. Str.
27	San Fernando, 02/09/71	6.6	reverse	LA Hollywood Stor Lot	90	NEHRP-D/ Geomatrix D	21.2 (fault)	0.210	Free Field / Instr. Str.
28	San Fernando, 02/09/71	6.6	reverse	LA Hollywood Stor Lot	180	NEHRP-D/ Geomatrix D	21.2 (fault)	0.174	Free Field / Instr. Str.

TABLE 2.4 (Cont'd)

Record #	Earthquake	Magnitude (M)	Fault	Station	Component	Site Classification	Distance (d) (km)	PGA (g)	Instrument Housing
	Strong Ground Motion data from PEER								
29	Superstition Hills (A), 11/24/87	6.3	strike-slip	Wildlife Liquef. Array	90	Geomatrix D	24.7 (fault)	0.132	Free Field / Instr. Str.
30	Superstition Hills (A), 11/24/87	6.3	strike-slip	Wildlife Liquef. Array	360	Geomatrix D	24.7 (fault)	0.134	Free Field / Instr. Str.
31	Superstition Hills (B), 11/24/87	6.7	strike-slip	Wildlife Liquef. Array	90	Geomatrix D	24.4 (fault)	0.181	Free Field / Instr. Str.
32	Superstition Hills (B), 11/24/87	6.7	strike-slip	Wildlife Liquef. Array	360	Geomatrix D	24.4 (fault)	0.207	Free Field / Instr. Str.
33	Taiwan Smart1 (40), 05/20/86	6.4	reverse	Smart1 M07	NS	Geomatrix D	64.0 (fault)	0.254	Free Field / Instr. Str.
34	Taiwan Smart1 (40), 05/20/86	6.4	reverse	Smart1 M07	EW	Geomatrix D	64.0 (fault)	0.182	Free Field / Instr. Str.
35	Taiwan Smart1 (45), 11/14/86	7.3	reverse	Smart1 O02	NS	Geomatrix D	39.0 (fault)	0.242	Free Field / Instr. Str.
36	Taiwan Smart1 (45), 11/14/86	7.3	reverse	Smart1 O02	EW	Geomatrix D	39.0 (fault)	0.160	Free Field / Instr. Str.
37	Taiwan Smart1 (5), 01/29/81	6.3	reverse	Smart1 I12	NS	Geomatrix D	21.0 (fault)	0.113	Free Field / Instr. Str.
38	Taiwan Smart1 (5), 01/29/81	6.3	reverse	Smart1 I12	EW	Geomatrix D	21.0 (fault)	0.140	Free Field / Instr. Str.
39	Victoria / Mexico, 06/09/80	6.4	strike-slip	Chihuahua	102	NEHRP-D/ Geomatrix D	36.6 (hypo)	0.150	Free Field / Instr. Str.
40	Victoria / Mexico, 06/09/80	6.4	strike-slip	Chihuahua	192	NEHRP-D/ Geomatrix D	36.6 (hypo)	0.092	Free Field / Instr. Str.
41	Whittier Narrows, 10/01/87	6.0	reverse-oblique	LA Hollywood Stor FF	0	NEHRP-D/ Geomatrix D	25.2 (fault)	0.221	Free Field / Instr. Str.
42	Whittier Narrows, 10/01/87	6.0	reverse-oblique	LA Hollywood Stor FF	90	NEHRP-D/ Geomatrix D	25.2 (fault)	0.124	Free Field / Instr. Str.

TABLE 2.4 (Cont'd)

Record #	Earthquake	Magnitude (M)	Fault	Station	Component	Site Classification	Distance (d) (km)	PGA (g)	Instrument Housing
	Strong Ground Motion data from PEER								
43	Chalfant Valley, 07/21/86	6.2	strike-slip	Benton	270	Geomatrix D	37.2 (fault)	0.209	1-Story Building
44	Chalfant Valley, 07/21/86	6.2	strike-slip	Benton	360	Geomatrix D	37.2 (fault)	0.177	1-Story Building
45	Duzce / Turkiye, 11/12/99	7.1	strike-slip	Duzce	180	NEHRP-D/ Geomatrix D	8.2 (fault)	0.348	1-Story Building
46	Duzce / Turkiye, 11/12/99	7.1	strike-slip	Duzce	270	NEHRP-D/ Geomatrix D	8.2 (fault)	0.535	1-Story Building
47	Kocaeli / Turkiye, 08/17/99	7.4	strike-slip	Duzce	180	NEHRP-D/ Geomatrix D	12.7 (fault)	0.312	1-Story Building
48	Kocaeli / Turkiye, 08/17/99	7.4	strike-slip	Duzce	270	NEHRP-D/ Geomatrix D	12.7 (fault)	0.358	1-Story Building
49	Superstition Hills (B), 11/24/87	6.7	strike-slip	Salton Sea Wildlife Ref.	225	NEHRP-E/ Geomatrix D	27.1 (fault)	0.119	1-Story Building
50	Superstition Hills (B), 11/24/87	6.7	strike-slip	Salton Sea Wildlife Ref.	315	NEHRP-E/ Geomatrix D	27.1 (fault)	0.167	1-Story Building
51	Westmorland, 04/26/81	5.8	strike-slip	Salton Sea Wildlife Ref.	225	NEHRP-E/ Geomatrix D	10.1 (hypo)	0.199	1-Story Building
52	Westmorland, 04/26/81	5.8	strike-slip	Salton Sea Wildlife Ref.	315	NEHRP-E/ Geomatrix D	10.1 (hypo)	0.176	1-Story Building

TABLE 2.4 (Cont'd)

Record #	Earthquake	Magnitude (M)	Fault	Station	Component	Site Classification	Distance (d) (km)	PGA (g)	Instrument Housing
	Strong Ground Motion data from COSMOS								
53	Big Bear, 06/28/92	6.4	strike-slip	San Bernardino - 2nd Arrowhead	270	Deep Alluvium	44.5 (hypo)	0.111	Free Field / Instr. Str.
54	Big Bear, 06/28/92	6.4	strike-slip	San Bernardino - 2nd Arrowhead	360	Deep Alluvium	44.5 (hypo)	0.095	Free Field / Instr. Str.
55	Hokkaido / Japan '04, 12/06/04	6.7	unknown	Shibetsu	NS	Soft Soil	92.1 (hypo)	0.115	Ground
56	Hokkaido / Japan '04, 12/06/04	6.7	unknown	Shibetsu	EW	Soft Soil	92.1 (hypo)	0.238	Ground
57	Hokkaido / Japan '05, 01/18/05	6.3	unknown	Betsukai	NS	Soft Soil	69.8 (hypo)	0.134	Ground
58	Hokkaido / Japan '05, 01/18/05	6.3	unknown	Betsukai	EW	Soft Soil	69.8 (hypo)	0.121	Ground
59	Loma Prieta, 10/18/89	6.9	oblique	San Francisco Int.Airport	0	Deep Alluvium	48.5 (fault)	0.235	1-Story Building
60	Loma Prieta, 10/18/89	6.9	oblique	San Francisco Int.Airport	90	Deep Alluvium	48.5 (fault)	0.332	1-Story Building
61	Near South Coast of Honshu / Japan, 03/16/97	5.8	unknown	Tsukude	NS	Soft Soil	40.4 (hypo)	0.535	Ground
62	Near South Coast of Honshu / Japan, 03/16/97	5.8	unknown	Tsukude	EW	Soft Soil	40.4 (hypo)	0.390	Ground
63	Northridge, 01/17/94	6.7	thrust/reverse	Santa Monica City Hall Grounds	90	Alluvium	27.4 (fault)	0.883	Free Field / Instr. Str.
64	Northridge, 01/17/94	6.7	thrust/reverse	Santa Monica City Hall Grounds	360	Alluvium	27.4 (fault)	0.370	Free Field / Instr. Str.

TABLE 2.4 (Cont'd)

Record #	Earthquake	Magnitude (M)	Fault	Station	Component	Site Classification	Distance (d) (km)	PGA (g)	Instrument Housing
	Strong Ground Motion data from COSMOS								
65	Parkfield, 09/28/04	6.0	strike-slip	Cholame 1E	90	Alluvium	7.9 (fault)	0.427	Free Field / Instr. Str.
66	Parkfield, 09/28/04	6.0	strike-slip	Cholame 1E	360	Alluvium	7.9 (fault)	0.343	Free Field / Instr. Str.
67	Southern Honshu / Japan, 06/25/97	6.1	unknown	Hagi	NS	Soft Soil	31.8 (hypo)	0.127	Ground
68	Southern Honshu / Japan, 06/25/97	6.1	unknown	Hagi	EW	Soft Soil	31.8 (hypo)	0.100	Ground
69	Tokachi-Oki / Japan, 09/26/03	8.0	unknown	Chokubetsu	NS	Soft Soil	116.8 (hypo)	0.753	Ground
70	Tokachi-Oki / Japan, 09/26/03	8.0	unknown	Chokubetsu	EW	Soft Soil	116.8 (hypo)	0.800	Ground
71	Whittier Narrows, 10/01/87	6.1	thrust/reverse	Long Beach, Rancho Los Cerritos	0	Deep Alluvium	27.1 (fault)	0.238	Free Field / Instr. Str.
72	Whittier Narrows, 10/01/87	6.1	thrust/reverse	Long Beach, Rancho Los Cerritos	90	Deep Alluvium	27.1 (fault)	0.147	Free Field / Instr. Str.

Instr.Str. : Instrument Shelter
fault : to the fault rupture
hypo : hypocentral

TABLE 2.5 – The list of earthquakes on rock sites

Record #	Earthquake	Magnitude (M)	Fault	Station	Component	Site Classification	Distance (d) (km)	PGA (g)	Instrument Housing
	Strong Ground Motion data from COSMOS & PEER								
1	Cape Mendocino, 04/25/92	7.1	thrust/reverse	89005 Cape Mendocino	0	NEHRP-B/Geomatrix A	8.5 (fault)	1.497	Free Field / Instr. Str.
2	Cape Mendocino, 04/25/92	7.1	thrust/reverse	89005 Cape Mendocino	90	NEHRP-B/Geomatrix A	8.5 (fault)	1.039	Free Field / Instr. Str.
3	Landers, 06/28/92	7.3	strike-slip	Silent Valley–Poppet Flat	0	NEHRP-B/Geomatrix A	51.7 (fault)	0.050	Free Field / Instr. Str.
4	Landers, 06/28/92	7.3	strike-slip	Silent Valley–Poppet Flat	90	NEHRP-B/Geomatrix A	51.7 (fault)	0.040	Free Field / Instr. Str.
5	Northridge, 01/17/94	6.7	thrust/reverse	Mt. Wilson -CIT Seis. Sta.	0	NEHRP-B/Geomatrix A	36.1 (fault)	0.234	Free Field / Instr. Str.
6	Northridge, 01/17/94	6.7	thrust/reverse	Mt. Wilson -CIT Seis. Sta.	90	NEHRP-B/Geomatrix A	36.1 (fault)	0.134	Free Field / Instr. Str.
7	San Fernando, 02/09/71	6.6	reverse	Lake Hughes Array #4	111	Weathered Granite	23.8 (fault)	0.171	Free Field / Instr. Str.
8	San Fernando, 02/09/71	6.6	reverse	Lake Hughes Array #4	201	Weathered Granite	23.8 (fault)	0.154	Free Field / Instr. Str.

Instr.Str. : Instrument Shelter
fault : to the fault rupture

CHAPTER 3

RESULTS OF ANALYSES

3.1 The significance of frequency-dependency of impedance coefficients for a linear structure

The dimensionless SSI parameters $\bar{s}$ and $\bar{h}$ reflect the significance of inertial interaction on structural response. Sets of analyses that consider a linear structure are performed. In the first set of analyses, $\bar{s}$ takes values within the range of 0.5 - 2.0, $\bar{h}$ is set to 1.0 constantly, and ω_n ($=2\pi/T_n$) is considered as representative frequency of excitation. The ratio of maximum absolute structural distortion computed with frequency-independent impedance coefficients ($u_{max}(\omega_n)$) to that computed with frequency-dependent impedance coefficients ($u_{max}(\omega)$) is investigated. The variation of displacement ratio ($u_{max}(\omega_n) / u_{max}(\omega)$) for a range of T_n is plotted in Figures 3.1.a-d. The solid line plotted in these figures shows the variation of mean displacement ratio, and the dashed lines delineate two standard deviations interval around the mean.

The mean value of the displacement ratio is around 1.0 for the case $\bar{s} = 0.5$ (Figure 3.1.a). However, it decreases to about 0.95 and 0.9 as $\bar{s}$ increases to 1.5 and 2.0, respectively (Figure 3.2). Hence, as the structure becomes stiffer and the soil becomes softer, the inertial interaction becomes more significant, and the results are more sensitive to the frequency-dependency of foundation impedance. Besides, the difference between the flexible-base and fixed-base fundamental period of a structure increases with increasing $\bar{s}$, and T_n becomes a poorer representative for structural oscillations. Therefore, the use of fixed-base fundamental period of a

structure for the estimation of frequency-independent foundation impedance coefficients can result in unconservative results. But, the reduction in the mean displacement ratio is at most 10% for the range of $\bar{s}$ considered in the analyses.

The variation of standard deviation of displacement ratio with T_n and $\bar{s}$ is shown in Figure 3.3. The dispersion of displacement ratio around the mean increases with the parameter $\bar{s}$, but is not sensitive to T_n.

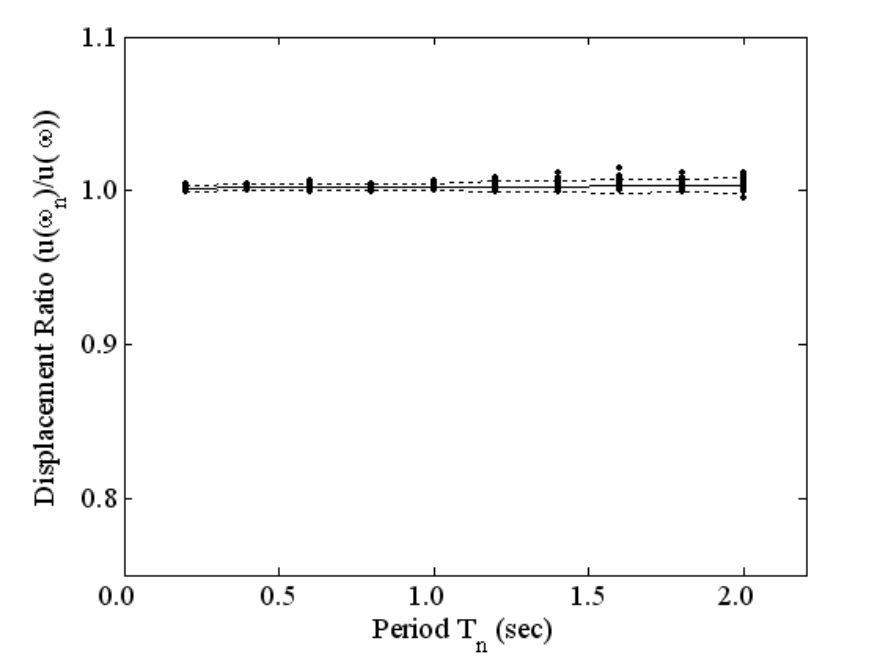

(a)

Figure 3.1 – Displacement Ratio for $\bar{h} = 1.0$, and (a) $\bar{s} = 0.5$, (b) $\bar{s} = 1.0$, (c), $\bar{s} = 1.5$, and (d) $\bar{s} = 2.0$.

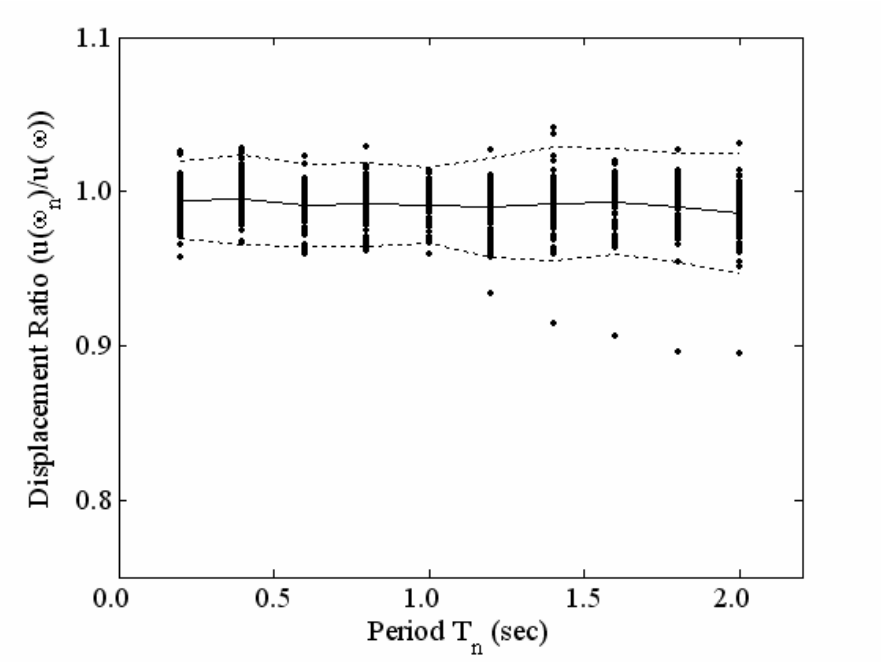

(b)

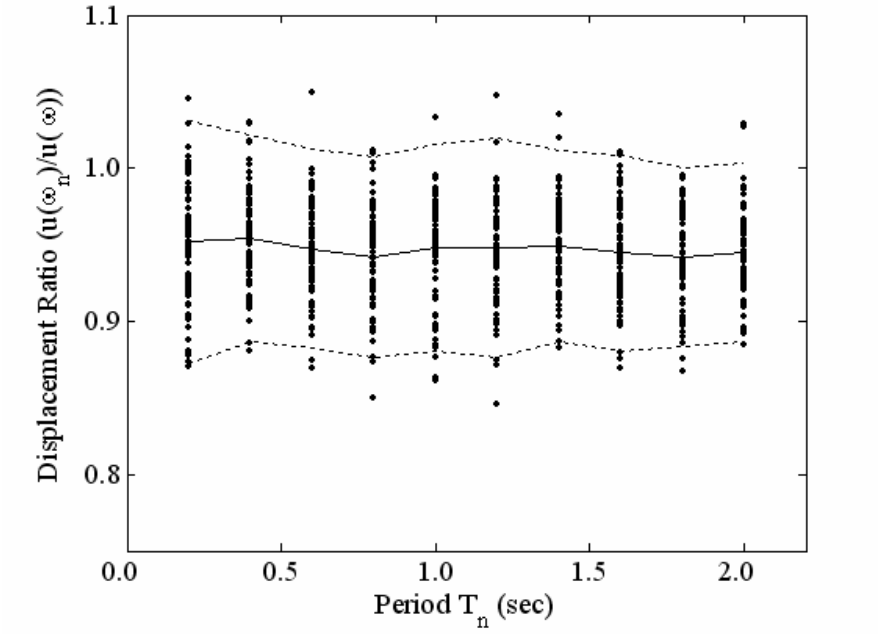

(c)

Figure 3.1 – Continued

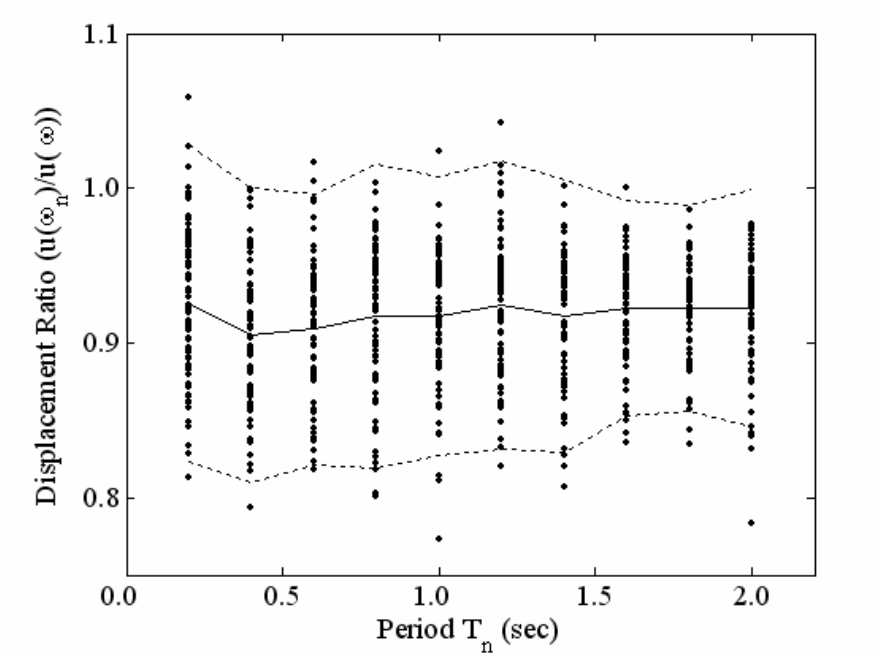

(d)

Figure 3.1 – Continued

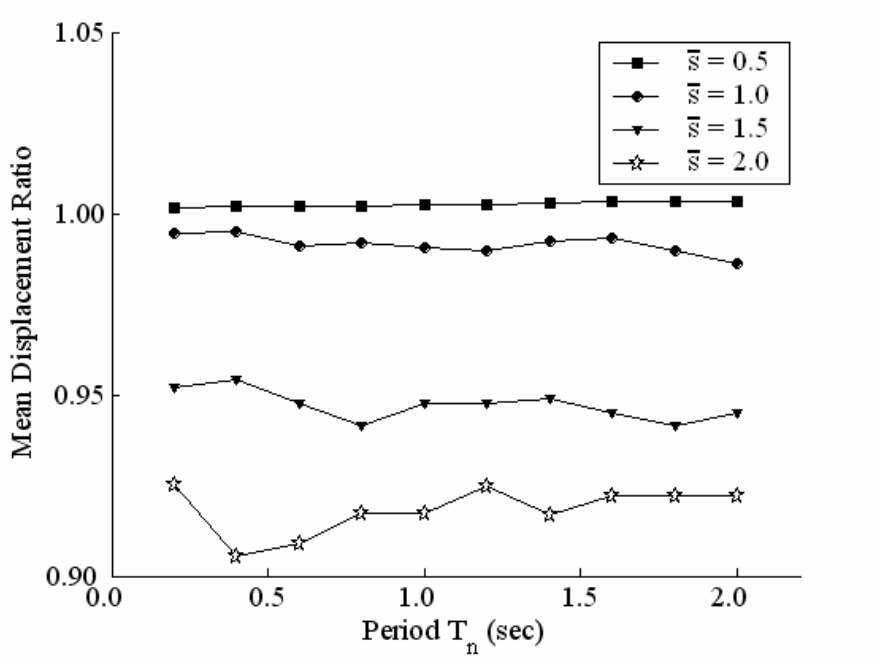

Figure 3.2 – Mean displacement ratios for different values of $\bar{s}$, and $\bar{h} = 1.0$.

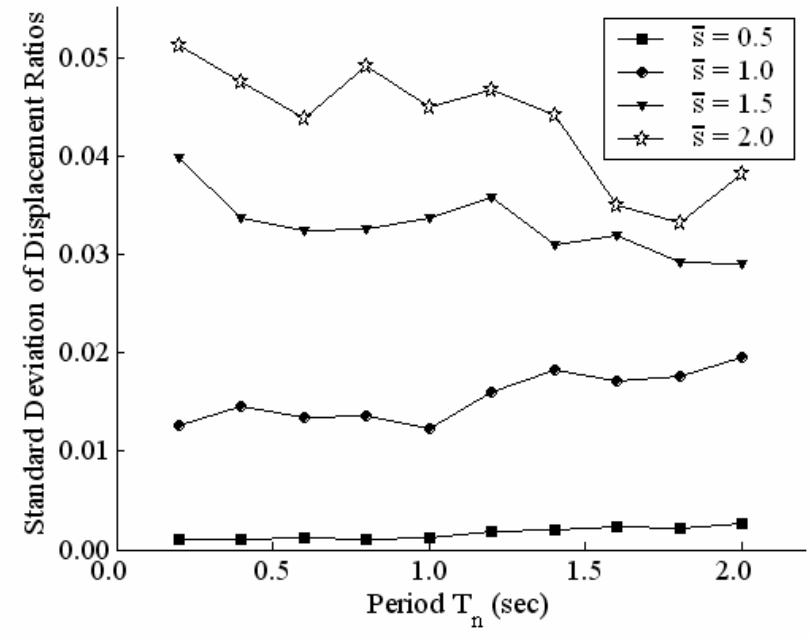

Figure 3.3 – Standard deviation of displacement ratios for different values of $\bar{s}$, and $\bar{h} = 1.0$.

In the second set of analyses, $\bar{s}$ is set to 1.0 constantly, but the slenderness ratio, $\bar{h}$, varies within the range from 0.5 to 2.0. Figures 3.4.a-d present the variation of the displacement ratio ($u_{max}(\omega_n)$ / $u_{max}(\omega)$) by T_n. The results indicate a trend of increasing displacement ratio with increasing $\bar{h}$, most possibly due to increasing contribution of rocking mode of foundation displacements in overall response of structure, which results in reduced damping ratio for the flexible-base structure.

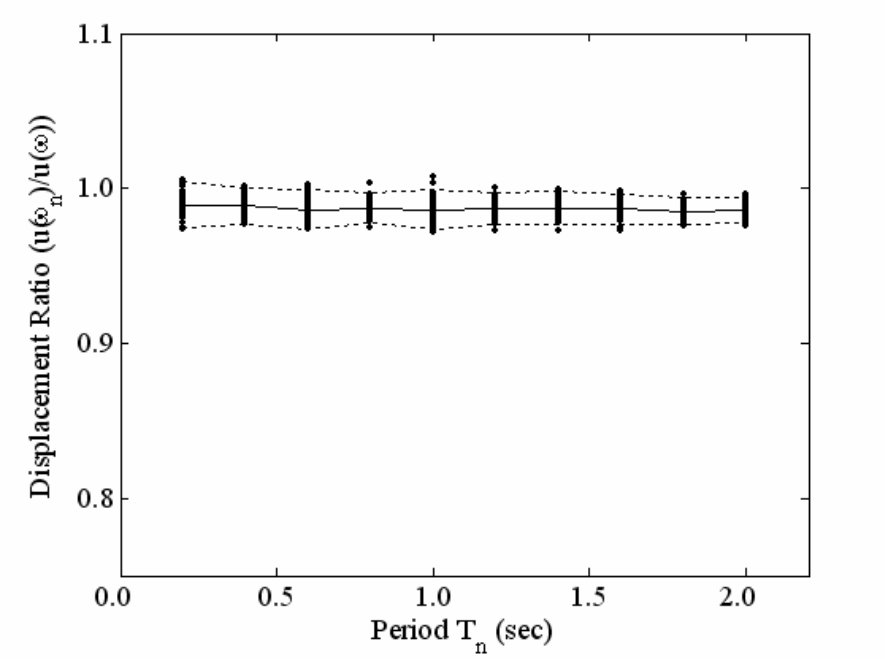

(a)

Figure 3.4 – Displacement ratio for $\bar{s} = 1.0$, and (a) $\bar{h} = 0.5$, (b) $\bar{h} = 1.0$, (c) $\bar{h} = 1.5$, and (d) $\bar{h} = 2.0$.

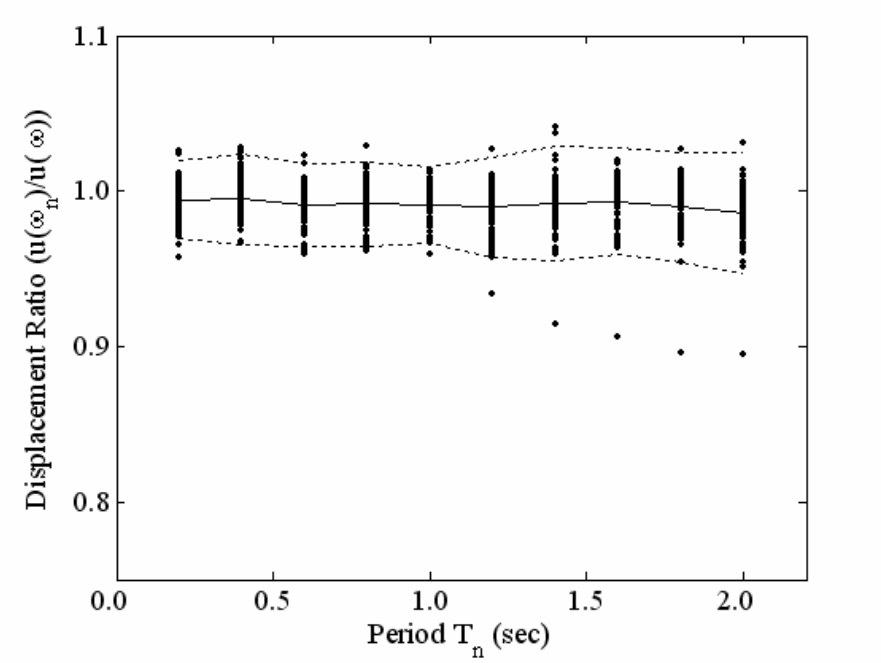

(b)

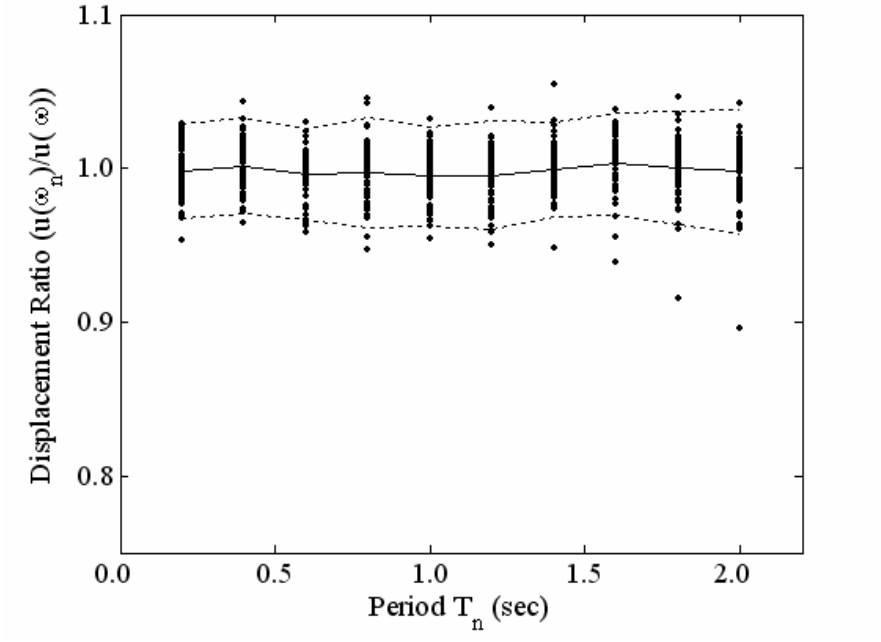

(c)

Figure 3.4 – Continued

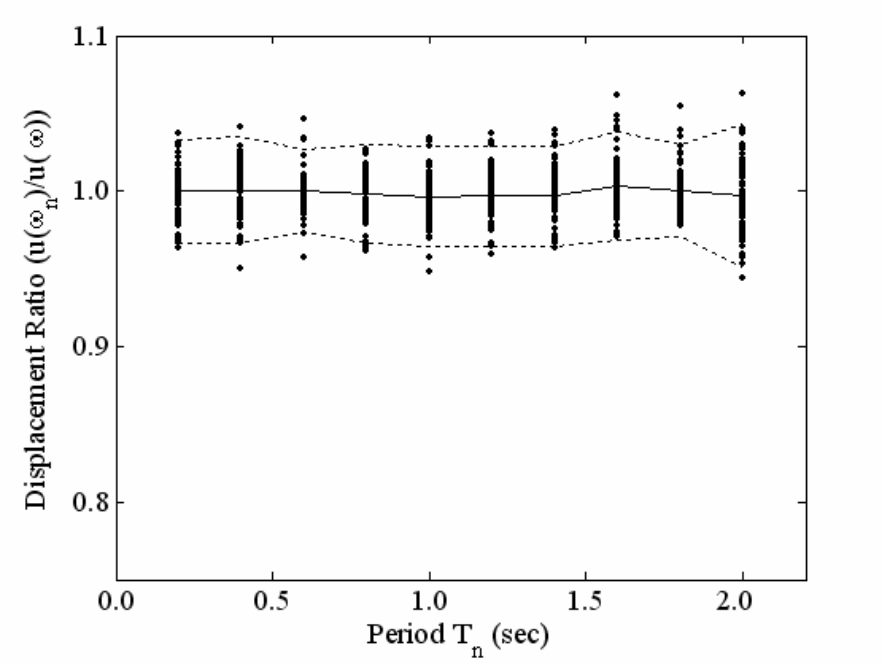

(d)

Figure 3.4 – Continued

Figure 3.5 shows the variation of mean displacement ratio with $\bar{h}$ and T_n. The computed mean is about 1.0, and the mean displacement ratio gets closer to 1.0 by increasing $\bar{h}$. Hence, the more slender the structures are, the more accurate the approximate inertial interaction analyses with frequency-independent foundation impedance are. Besides, the reduction in mean displacement ratio, and the increase in dispersion of displacements are less sensitive to $\bar{h}$ than $\bar{s}$.

The standard deviation of displacement ratio is not sensitive to $\bar{h}$, for the range $1.0 \leq \bar{h} \leq 2.0$ (Figure 3.6), but the least dispersion in results is obtained for $\bar{h}=0.5$. Hence, the dimensionless parameter $\bar{h}$ appears to be less critical than $\bar{s}$ for the inertial interaction analyses with frequency-independent foundation impedance.

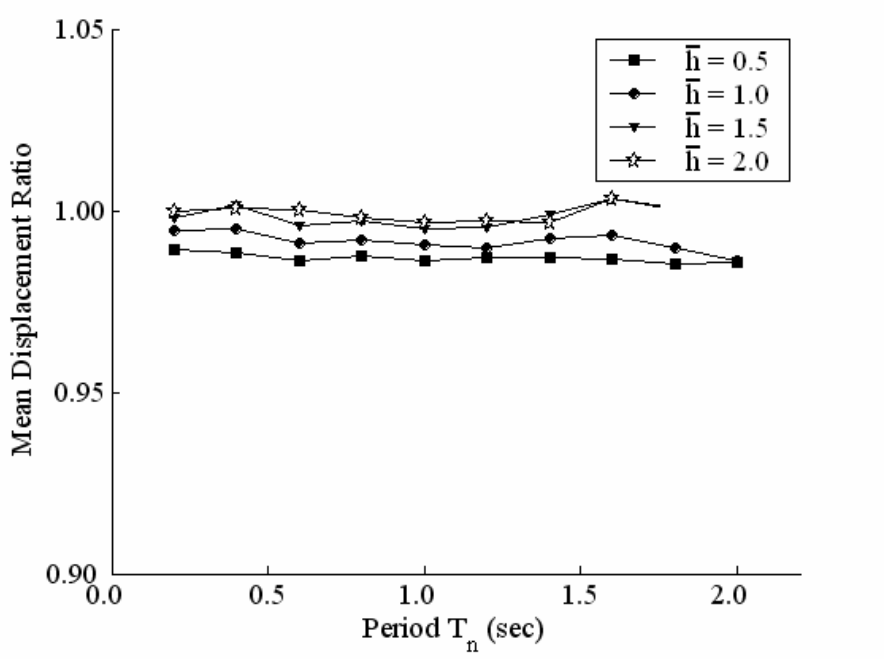

Figure 3.5 – Mean displacement ratios for different values of $\bar{h}$, and $\bar{s} = 1.0$

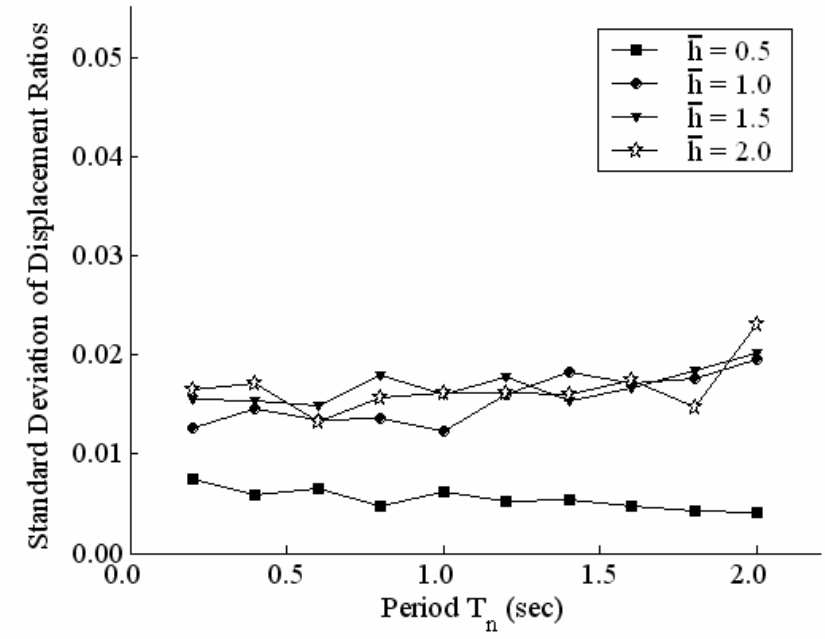

Figure 3.6 – Standard deviation of displacement ratio for different values of $\bar{h}$, and $\bar{s} = 1.0$

Figure 3.7 and 3.8 show the variation of the mean displacement ratio and the standard deviation of mean displacement ratio by $\bar{s}$ and T_n, under constant $\bar{h}$=2.0. The mean displacement ratio decreases as $\bar{s}$ increases for a given T_n. Results for the mean displacement ratio are generally similar to previous results for $\bar{h}$=1.0. However, for the case $\bar{s}$=2.0 and h=2.0, the mean displacement ratios are apparently lower than those for $\bar{s}$=2.0 and h=1.0. Moreover, dispersions of the displacement ratio for the cases with $\bar{h}$=2.0 are more emphasized than those for the cases with $\bar{h}$=1.0 (Figure 3.3), although the ratio of flexible period to fixed of structure ($\tilde{T}/T$) does not dramatically change between $\bar{h}$=1.0 and $\bar{h}$=2.0 for a given $\bar{s}$ (Figure 2.4). The significant increase in the dispersion of results can be related to the increase in $\bar{m}$ parameter as well. An increase in $\bar{h}$ results in an equal increase in $\bar{m}$, since the two parameters are assumed to be equal to each other in the analyses.

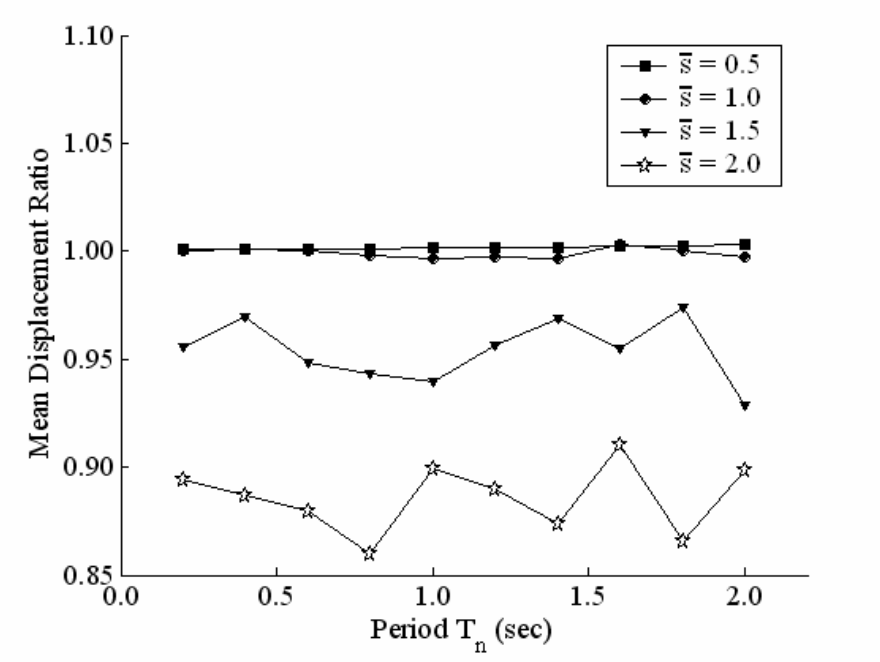

Figure 3.7 – Mean displacement ratios for different values of $\bar{s}$, and $\bar{h} = 2.0$.

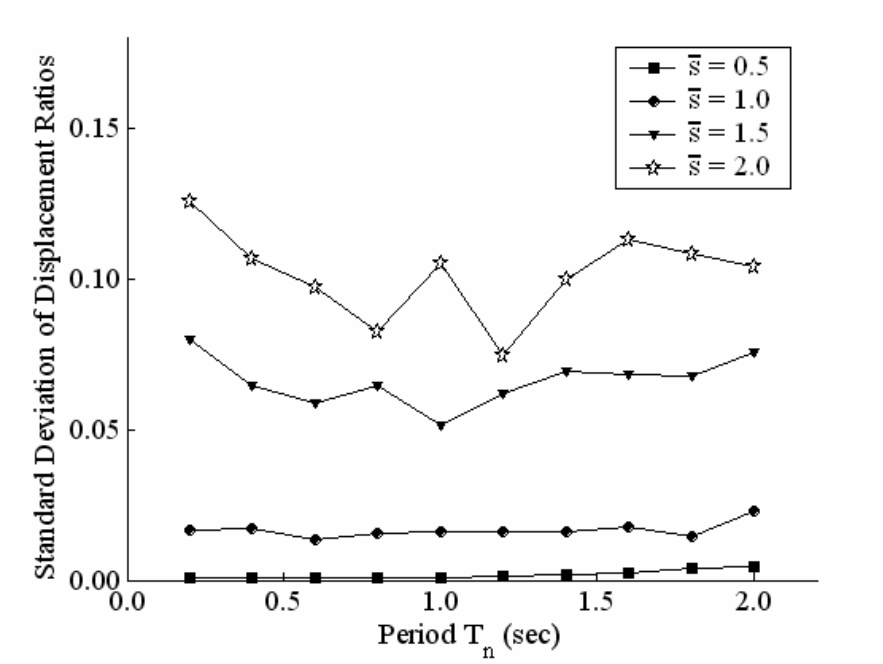

Figure 3.8 – Standard deviation of displacement ratio for different values of $\bar{s}$, and $\bar{h} = 2.0$.

Figure 3.9 displays the variation of mean displacement ratio for earthquake records on rock sites. The analyses are conducted for a variable $\bar{s}$ and a constant $\bar{h}$, set to 1.0. Comparing Figure 3.9 with Figure 3.2, it is concluded that the effect of rock sites and soil sites on the accuracy of the frequency-independent impedance calculations does not differ much. Considering the significant difference between the shapes of mean normalised spectrum of soil-site records (Figure 2.6) and rock-site records (Figure 2.7), it is concluded that the reduction in displacement ratio is not very sensitive to the site conditions of the records employed in analyses.

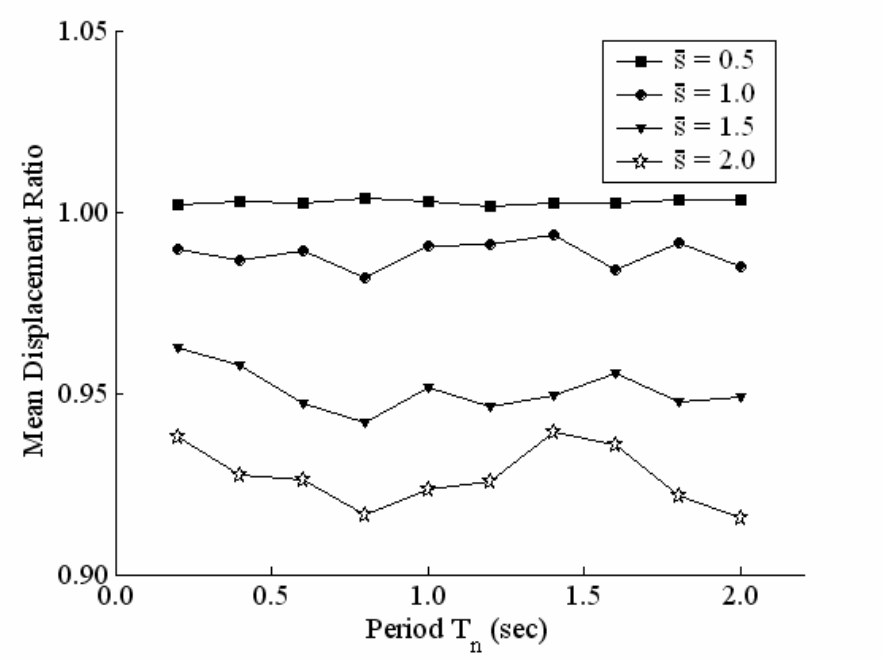

Figure 3.9 – Mean displacement ratios of earthquake records on rock sites for different values of $\bar{s}$, and $\bar{h} = 1.0$

3.2 Effects of Poisson's Ratio and Soil Damping on Results

In addition to the dimensionless parameters $\bar{s}$ and $\bar{h}$, the effect of the Poisson's ratio, ν, and the soil damping ratio, ξ_g, on previously obtained results is investigated by a set of analyses. For these sets of analyses, the dimensionless parameters $\bar{s}$ and $\bar{h}$ are set to 2.0 and 1.0 respectively. The variation of mean and standard deviation of displacement ratio for a structure on soil with $\nu = 0.3$ and $\nu = 0.5$, which are representative for drained and undrained soil behaviour respectively, are compared in Figures 3.10.a-b. It is observed that Poisson's ratio of soil has no significant effect on the accuracy and precision of inertial interaction analyses with frequency-independent impedance coefficients.

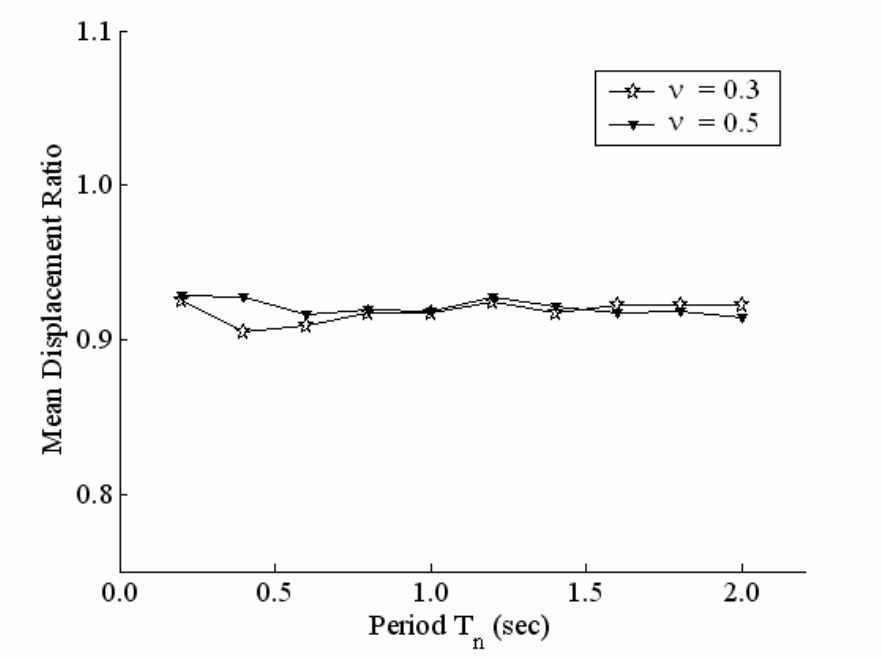

(a)

Figure 3.10 – Comparison of (a) mean and (b) standard deviation of displacement ratio for $\nu = 0.3$ and $\nu = 0.5$.

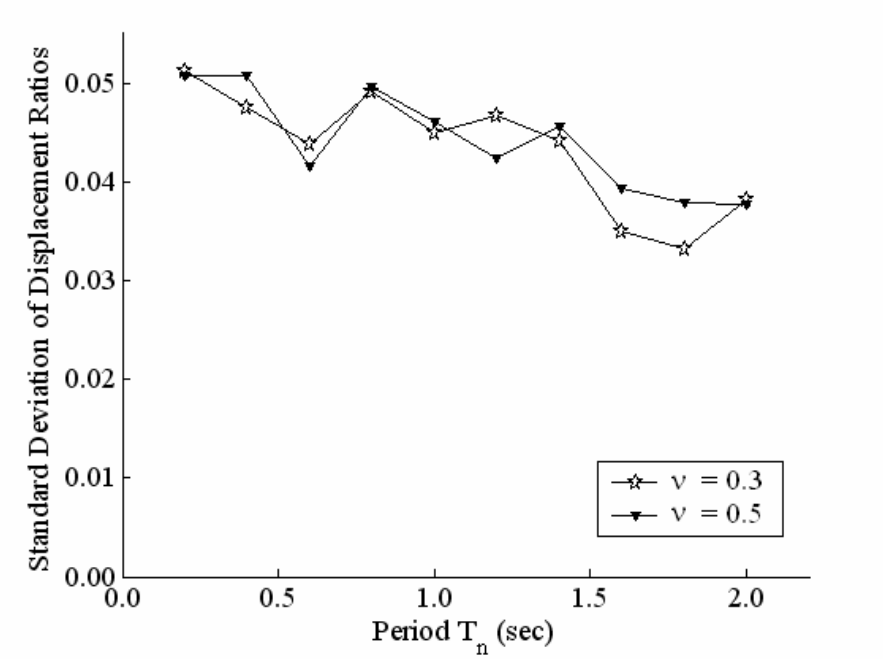

(b)

Figure 3.10 – Continued

In order to investigate the effect of soil damping due to hysteretic response of soils, the correspondence principle is employed. The variation of mean and standard deviation of the displacement ratio for ξ_g=0%, 5%, 10%, and 15% is shown in Figures 3.11.a-b. It is observed that the displacement ratio is almost insensitive to the damping ratio of soil, but the dispersion of results decreases as the damping ratio of soil increases.

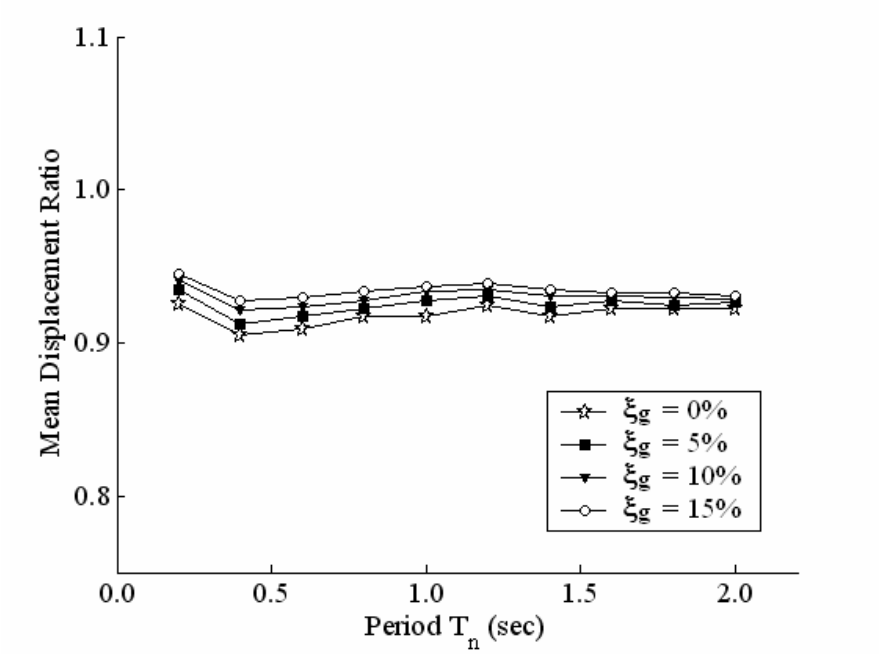

(a)

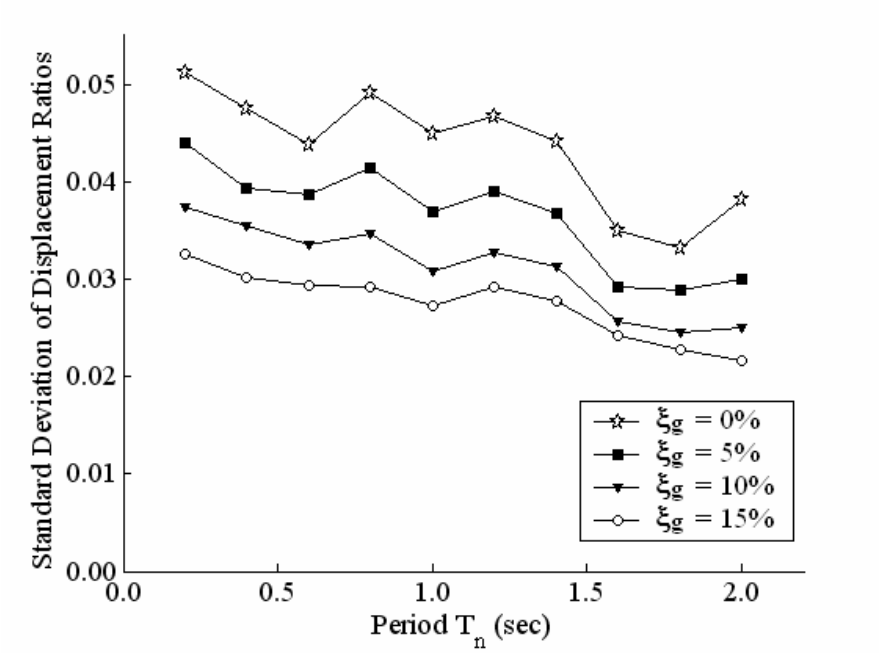

(b)

Figure 3.11 – Comparison of (a) mean and (b) standard deviation of displacement ratio for ξ_g = 0%, 5%, 10%, and 15%.

3.3 The significance of frequency-dependency of impedance coefficients for a nonlinear structure

In order to provide insight to accuracy and precision of nonlinear structural response analyses in which inertial interaction is approximately considered with frequency-independent foundation impedance coefficients, a set of analyses with $\bar{s} = 2.0$ and $\bar{h} = 1.0$ is performed. Similar to the work done for previous sections, the natural period of the structure (T_n) that is pertinent to elastic response is employed for the calculation of impedance coefficients. This is due to the fact that, in practical applications, T_n is a well-defined parameter that can be estimated by reliable empirical expressions provided for regular structures, or through modal analysis. The equivalent linearization approach is used for the approximation of nonlinear structural response. The values of effective period and damping ratio that correspond to $\mu = 1$ (i.e., elastic), $\mu = 4$ and $\mu = 7$ are considered in the analyses.

Considering different levels of nonlinear response, the variation of mean and standard deviation of the displacement ratio by T_n is presented in Figures 3.12.a-b. Although a slight improvement on mean displacement ratio appears, no significant difference between the results for cases of nonlinear and linear structural response is obtained. This is explained by the fact that, although the natural period of fixed-base elastic response can be a poor estimator for the effective period of a nonlinear structure on flexible base, the foundation flexibility is less significant for the nonlinear structural response than the linear structural response. In other words, for a given set of dimensionless SSI parameters pertinent to elastic response of a structure, the increase in flexibility and damping of structure due to its nonlinear response results in a more pronounced contribution of structural parameters in overall response of soil-structure system. Therefore, the conclusions obtained for linear structural response are acceptable for the cases that nonlinear structural response is considered.

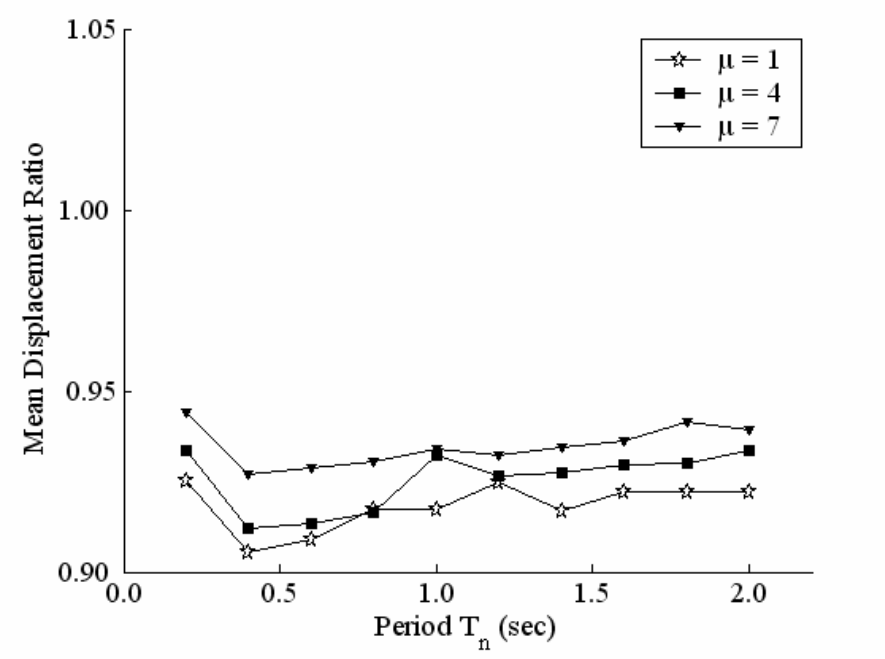

(a)

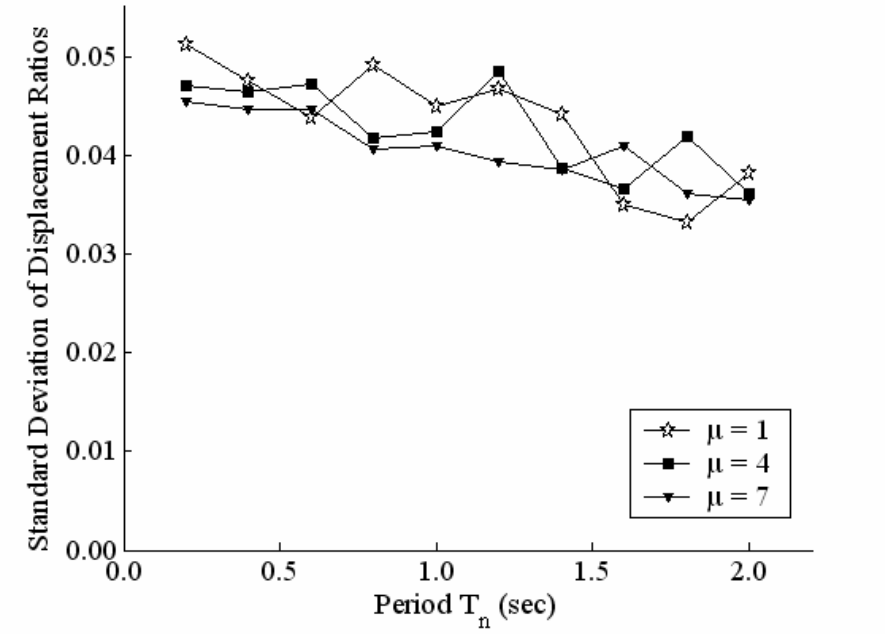

(b)

Figure 3.12 – Comparison of (a) mean and (b) standard deviation of displacement ratios pertinent to nonlinear structural response .

3.4 The effect of spectral shape on the dispersion of displacement ratio

The investigation of two typical records that indicate a small and a large dispersion in results provides more specific information on the subject matter. Therefore, two records are chosen in order to study the significance of spectral shape on dispersion of displacement ratio. The NS component of the Parkfield Earthquake record (09/28/04), and EW component of the Landers (06/28/92) Earthquake record are employed for the purpose. Figures 3.13 and 3.14 present the (5% damping) acceleration and displacement spectra of the records.

The Parkfield Earthquake record shows a much smoother spectrum than that of the Landers Earthquake record. The spectral acceleration decreases faster in long period range for the Parkfield record, hence a wide constant spectral displacement plateau exists for this record on periods greater than 0.5. However, the variation of spectral acceleration is more erratic for the Landers record.

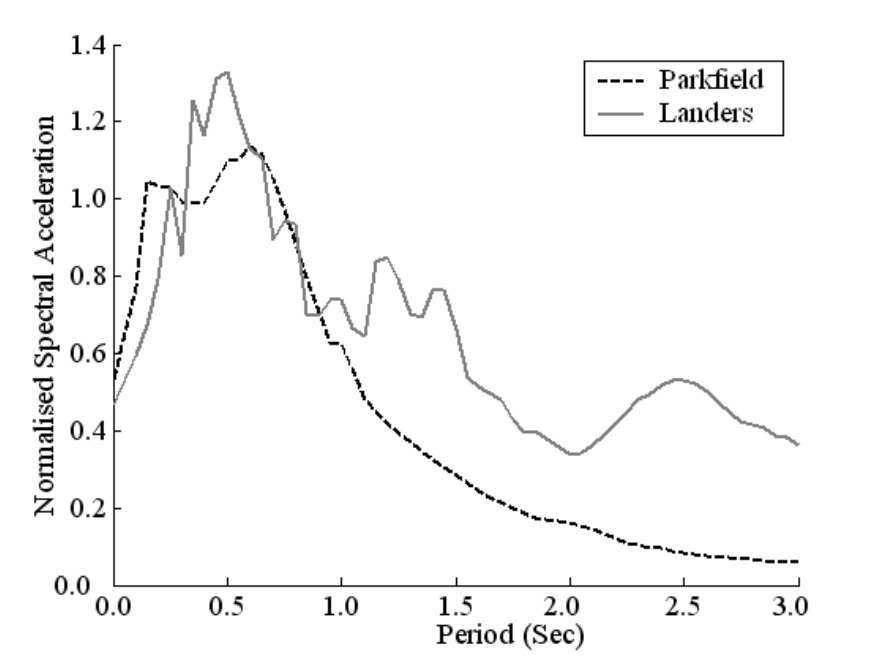

Figure 3.13 – Parkfield (09/28/04) Earthquake NS Component and Landers (06/28/92) Earthquake EW Component Acceleration Spectra

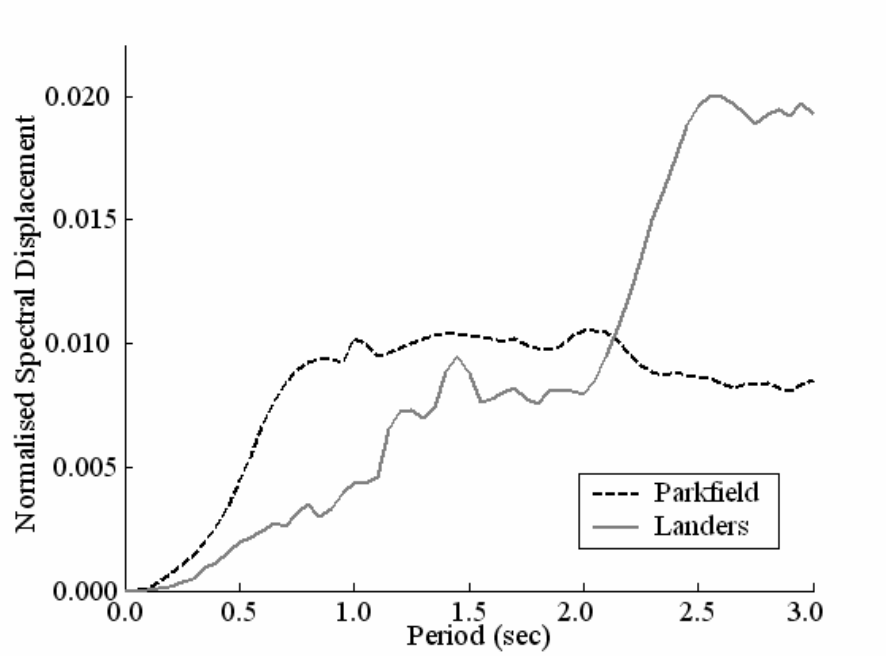

Figure 3.14 – Parkfield (09/28/04) Earthquake NS Component and Landers (06/28/92) Earthquake EW Component Displacement Spectra

Figure 3.15 presents the variation of the displacement ratio by $\bar{s}$, for the Parkfield record. The displacement ratio is relatively insensitive to T_n. The displacement ratio decreases by increasing $\bar{s}$, possibly due to overestimation of effective damping of the structure on flexible base. Therefore, the Parkfield record is a typical record that does not induce significant dispersion in error induced by the use of frequency-independent parameters.

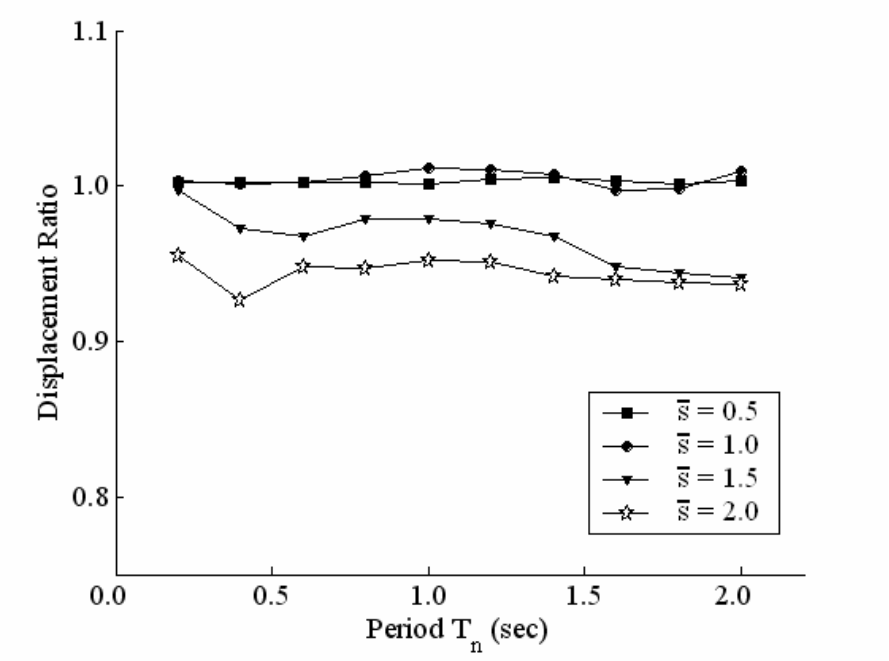

Figure 3.15 – The Response of Parkfield (09/28/04) Earthquake NS Component to $\bar{s}$

In contrast, the Landers record provides more scattered displacement ratio, as the inertial interaction becomes more significant (Figure 3.16). As $\bar{s}$ increases, the scattering of the displacement ratio around the average for the given range of T_n becomes more emphasized. Earthquake records with irregular spectrum shapes can amplify sensitivity of SSI analyses to parameters of interest. On the other hand, the insensitivity of mean displacement ratio to T_n in (Figure 3.2), is explained by the smoothness of the normalised mean spectra (Figure 2.6). Hence, a systematic selection of earthquake records is necessary in order to obtain justifiable variability in results of analyses.

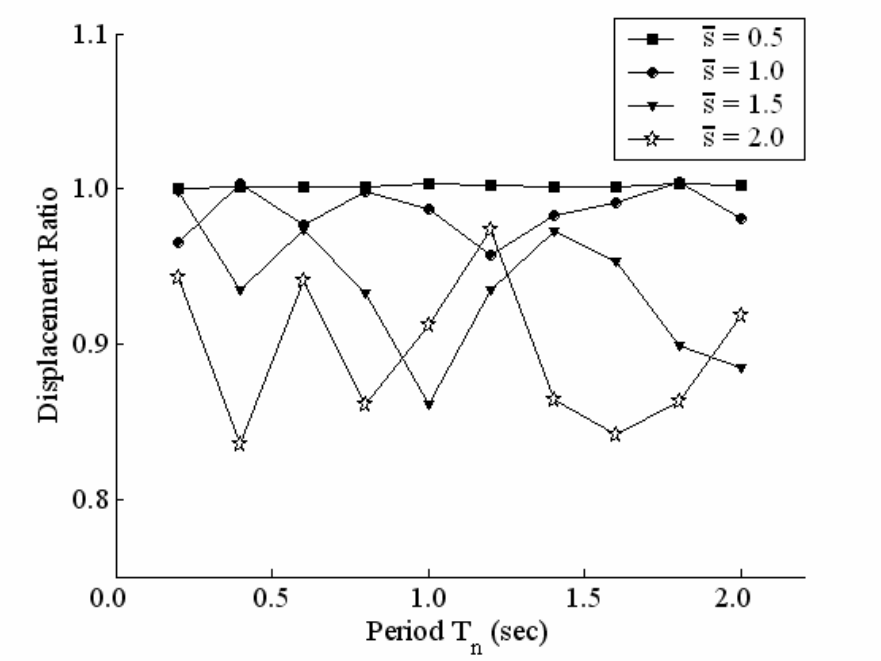

Figure 3.16 – The Response of Landers (06/28/92) Earthquake EW Component to $\bar{s}$

3.5 Utilisation of flexible-base structural period for calculation of frequency-independent impedance coefficients

In the previous sections, the natural period of the SDOF oscillator that represents the fixed-base structure is employed for calculation of frequency-independent foundation impedance coefficients. The mean error due to the ignorance of frequency-dependency of impedance coefficients is less than 10% for the range of dimensionless parameters considered in the analyses. However, in case that the natural period of the structure on flexible base ($\tilde{T}$) is used for calculation of frequency-independent foundation impedance coefficients, the resonance response of the structure on flexible base can be exactly computed. Hence, the period $\tilde{T}$ (or, the frequency $\tilde{\omega}$) can be used as the effective period of excitation in calculation of

impedance coefficients. An iterative approach for calculation of $\tilde{T}$ is necessary, since $\tilde{T}$ is also a function of foundation impedance coefficients. The dimensionless parameters $\bar{s}$ and $\bar{h}$ are set to 2.0 and 1.0 respectively for the analyses.

The comparison of the mean displacement ratios pertinent to $\tilde{T}$ and T_n is presented in Figure 3.17.a-b. The mean displacement ratio for the former period is closer to 1.0, implying a better representative period of excitation. However, when $\tilde{T}$ is employed, the dispersion of displacement ratio is significantly dependent on the fundamental period of structure.

When the effect of inertial interaction on structural response is moderate (i.e., $\bar{s} < 2.0$), the fundamental period of structure can be used for calculation of frequency-independent foundation impedance coefficients. However, when the response of flexible-base structure is considerably different from the response of fixed-base structure, use of $\tilde{T}$ can provide an improved approximation. That is, the use of $\tilde{T}$ instead of T_n is important for structures resting on very soft deposit, but the improvement on results may be compensated by the uncertainty inherent in determination of seismic loads for soft sites, as well as by the assumptions made for simplified SSI analyses.

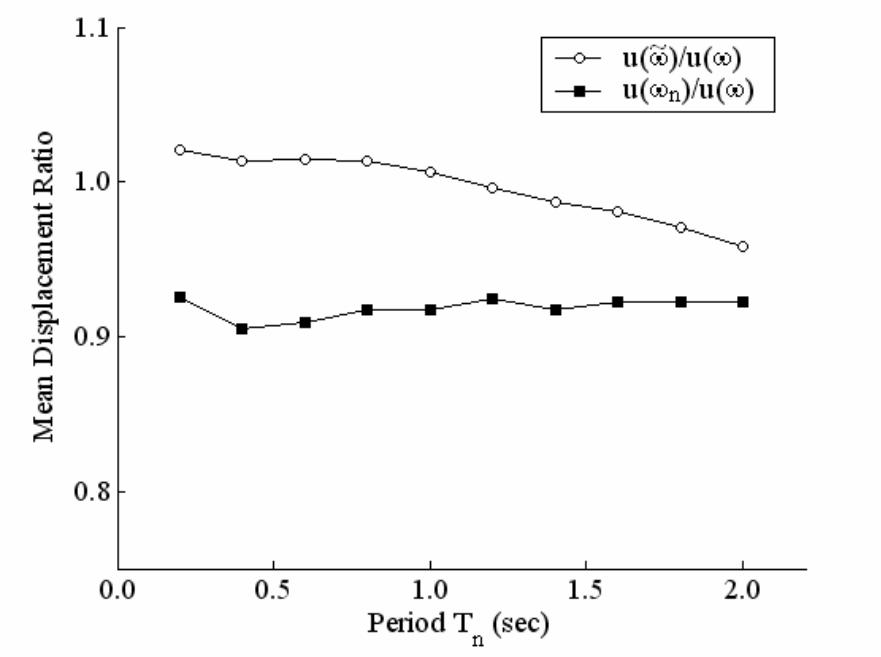

(a)

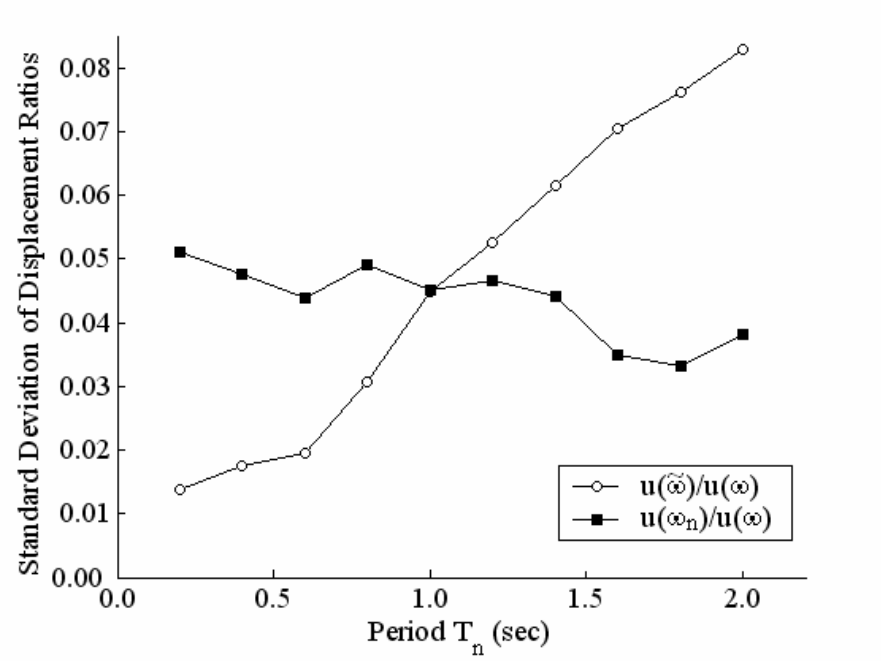

(b)

Figure 3.17 – Comparison of the (a) mean and (b) standard deviation of displacement ratio for the cases that $\tilde{\omega}$ or ω_n is employed for estimation of foundation impedance.

CHAPTER 4

SUMMARY AND CONCLUSIONS

4.1 Summary

This study focuses on the approximate analysis of inertial interaction between a structure and deformable soil, which increases damping and period of structural oscillations. The fundamental frequency of structure is substituted for excitation frequency term appearing in expressions for the dynamic shallow foundation impedance, in order to obtain frequency-independent stiffness and damping coefficients for an approximate soil-structure interaction analysis. The Ratio of maximum absolute structural distortions computed through considering frequency-dependent and frequency-independent foundation impedance coefficients is considered as an error indicator for approximation, and is referred as the displacement ratio in this study.

The frequency-dependent shallow foundation impedance is simulated by a simple model, namely the *Monkey-tail Model*. The model is composed of simple mass, spring and dashpot elements. The model parameters pertinent to a rigid disk foundation resting on surface of an elastic halfspace are employed, since the longest period elongation and the least increase in damping ratio for structural oscillations is obtained for the case of a surficial foundation. A linear SDOF oscillator with 5% viscous damping ratio simulates the structural response. A total of 72 acceleration histories, that are pertinent to two horizontal components of ground motion recorded on soil sites during 36 different events, are employed for dynamic response analyses.

A code is developed in order to solve the equations of motion for a structure on flexible base in frequency domain. The Fast Fourier Transform algorithm is employed for the dynamic response computations. The analyses are performed for a set of fixed-base structural period, and dimensionless SSI parameters. The code finally reports the displacement ratio, and plots the variation of the displacement ratio by structural period for each record.

The most significant dimensionless parameters that effect the accuracy of the approximate inertial interaction analyses are the slenderness ratio, $\bar{h}$, and the stiffness ratio, $\bar{s}$. The considered range of these parameters is from 0.5 to 2.0, so that the effect of inertial interaction on period of structural oscillations is moderate. In the initial set of analyses, the damping due to hysteretic response of soil is ignored, and the Poisson's ratio is set to 0.3. In the following analyses, the effect of hysteretic soil damping and Poisson's ratio on the results is investigated. Besides, the relationship between the dispersion of results and the smoothness of response spectrum is investigated through employing two particularly selected records.

Following the analyses based on the linear structural model, the validity of results for the cases that nonlinear structural response is considered is evaluated. Since the analyses are performed in frequency domain, equivalent linear approximation is used for structural response. Hence, the effective period and damping of a structure on which the ductility demand is 4 or 7 is used in analyses, whereas the natural structural period pertinent to linear fixed-base response is considered in calculation of foundation impedance coefficients. It is observed that, the conclusions regarding the accuracy and precision of approximate inertial interaction analyses are valid for the analyses consider nonlinear structural response.

Finally, it is shown that, the fundamental period of a structure on flexible base is a superior parameter to employ for the calculation of frequency-independent

impedance coefficients. However, calculation of the flexible-base period requires an iterative approach, since it is dependent on the frequency-dependent impedance coefficients, and the improvement is not significant when the role of inertial interaction is moderate.

4.2 Conclusions

Considering the limitations of the study, the following conclusions are reached for approximate inertial interaction analyses with frequency-independent foundation impedance coefficients:

- The fundamental period of structure can be used for calculation of frequency-independent foundation impedance coefficients when the effect of inertial interaction on structural response is moderate. However, the utilisation of $\tilde{T}$ produces an improved approximation for foundation impedance when the flexible-base response of a structure is considerably different from the fixed-base response.
- Use of earthquake records that produce erratic response spectrum shapes for dynamic inertial interaction analyses can amplify the sensitivity of seismic demand on structures to SSI parameters. The smoother the spectrum is, the more precise the approximation with frequency-independent foundation impedance is. Besides, the accuracy of approximation is not critically dependent on the site conditions of selected records for analyses.
- The hysteretic damping and Poisson's ratio of soil has no significant effect on the accuracy and precision of inertial interaction analyses with frequency-independent foundation impedance.

- The accuracy of approximate inertial interaction analyses is most sensitive to the dimensionless parameter $\bar{s}$. Hence, these analyses are less accurate for lower structural periods and softer ground conditions.
- The parameter $\bar{h}$ is less critical than $\bar{s}$ for the accuracy of inertial interaction analyses with frequency-independent foundation impedance coefficients. The approximate inertial interaction analyses are more conservative for slender structures, when $\bar{s}$ is constant.
- The nonlinearity of structural response does not improve or worsen the accuracy of approximate inertial interaction analyses with frequency-independent foundation impedance coefficients. When $\bar{s}$ is less than 2.0, the fundamental period of structure that is pertinent to its linear response can be considered as the effective excitation period for calculation of frequency-independent foundation impedance coefficients.

4.3 Future Study Recommendations

The following topics are recommended as future studies:

- Derivation of an improved formula to determine effective frequency for calculation of frequency-independent foundation impedance coefficients for the cases that the structural response is considerably nonlinear.
- Through employing transient response analyses for nonlinear structures, a comparison of seismic displacement demand on structures for the cases that a fixed-base structure, a flexible-base structure with frequency-independent foundation impedance, and a flexible-base structure with frequency-dependent foundation impedance are considered.
- An investigation of sensitivity of seismic displacement demand on structures to nonlinear response of foundation.

REFERENCES

Ambrosini, R. D., 2006. “Material damping vs. Radiation damping in soil-structure interaction analysis”, Computers and Geotechnics, 33, 86-92.

Avilés, J., and Pérez-Rocha, L. E., 1998. “Site effects and soil-structure interaction in the Valley of Mexico”, Soil Dynamics and Earthquake Engineering, 17, 29-39.

Avilés, J., and Pérez-Rocha, L. E., 1999. “Diagrams of effective periods and dampings of soil-structure systems”, Journal of Geotechnical and Geoenvironmental Engineering, 125(8), 711-715.

Avilés, J., and Pérez-Rocha, L. E., 2003. “Soil-structure interaction in yielding systems”, Earthquake Engineering Structural Dynamics, 32, 1748-1771.

Avilés, J., and Pérez-Rocha, L. E., 2005. “Design concepts for yielding structures on flexible foundation”, Engineering Structures, 27, 443-454.

Avilés, J., and Suárez, M., 2002. “Effective periods and dampings of building-foundation systems including seismic wave effects”, Engineering Structures, 24, 553-562.

Borcherdt, R. D., 1994. “Estimates of site dependent response spectra dor design (methodology and justification)”, Earthquake Spectra, Vol.10(4), 617-653.

CEN (Comité Européen de Normalisation) (2004). Eurocode 8: Design of structures for earthquake resistance. Part 5: Foundations, retaining structures and geotechnical aspects. EN 1998-5, Brussels, Belgium.

Ciampoli, M., and Pinto, P.E., 1995. "Effects of soil-structure interaction on inelastic seismic response of bridge piers", Journal of Structural Engineering, ASCE, 121(5), 806-814.

COSMOS, 2004. "COSMOS Virtual Data Center" Consortium of Organizations for Strong-Motion Observation Systems, http://db.cosmos-eq.org/, Last Accessed: November 2007

Dobry R., and Gazetas G., 1986. "Dynamis response of arbitrarily shaped foundations", Journal of Geotechnical Engineering, ASCE, 112(2), 109-135.

Elnashai, A. S., and McClure D. C., 1996. "Effect of modelling assumptions and input motion characteristics on seismic design parameters of RC bridge piers foundations", Earthquake Engineering Structural Dynamics, 25, 435-463.

Gazetas, G., 1991. "Formulas and charts for impedances of surface and embedded foundations", Journal of Geotechnical Engineering, ASCE, 117(9), 1363-1381.

Ghannad, M. A., and Jahankhah, H., 2007. "Site-dependent strength reduction coefficients for soil-structure systems", Soil Dynamics and Earthquake Engineering, 27, 99-110.

Iwan, W. D., 1980. "Estimating inelastic response spectra from elastic spectra", Earthquake Engineering Structural Dynamics, 8, 375-388

Kramer, S. L., 1996. "Geotechnical Earthquake Engineering", Prentice Hall 1996, 43pp.

Miranda, E., and Bertero V., 1994. “Evaluation of strength reduction coefficients of earthquake-resistant design”, Earthquake Spectra, 10(2), 357-379.

Mylonakis, G., and Gazetas, G., 2000. “Seismic soil-structure interaction: beneficial or detrimental?”, Journal of Earthquake Engineering, 4(3), 277-301.

NEHRP, 2003. “Recommended provisions for seismic regulations for new buildings and other structures (FEMA 450)” Parts 1 and 2, Building Seismic Safety Council, Washington D.C.

Nogami, T., Konagai, K. and Mikami, A., 2001. “Simple formulations of ground impedance functions for rigid surface foundations”, Soil Dynamics and Earthquake Engineering, 21, 475-484.

Pecker, A., and Pender, M., 2000. “Earthquake resistant design of foundations: new constructions”, Proceedings of GeoEng2000, 1, 313-332.

PEER, 2006. “PEER Strong Motion Database”, Pacific Earthquake Engineering Research Center, http://peer.berkeley.edu/smcat/, Last Accessed: November 2007

Saitoh, M., 2007. “Simple model of frequency-dependent impedance functions in soil-structure interaction using frequency-independent elements”, Journal of Engineering Mechanics, ASCE, 133(10), 1101-1114.

Şafak, E., 2006. “Time domain representation of frequency-dependent foundation impedance functions”, Soil Dynamics and Earthquake Engineering, 26, 65-70.

Takewaki, I., Takeda, N., Uetani, K., 2003. “Fast practical application of soil-structure interaction of embedded structures”, Soil Dynamics and Earthquake Engineering, 23, 195-202.

Veletsos, A. S., and Meek, J. W., 1974. “Dynamic behaviour of building foundation systems”, Journal of Earthquake Engineering Structural Dynamics, 3(2), 121-138.

Veletsos, A. S., and Nair, V. V., 1975. “Seismic interaction of structures on hysteretic foundations”, Journal of Earthquake Engineering, ASCE, 101(1), 109-129.

Veletsos, A. S., and Verbic, B., 1973. “Vibration of viscoelastic foundations”, Earthquake Engineering and Structural Dynamics, 2(1), 87-105.

Veletsos, A. S., and Verbic, B., 1974. “Basic response functions for elastic foundations”, Journal of the Engineering Mechanics Division, ASCE, 100, 189-202.

Veletsos, A. S., and Wei, Y. T., 1971. “Lateral and rocking vibration of footings”, Journal of the Soil Mechanics and Foundations Division, ASCE, 97, 1227-1248.

Wolf, J. P., 1985. “Dynamic Soil-Structure Interaction”, Prentice Hall 1985.

Wolf, J. P., and Somaini, D. R., 1986. “Approximate dynamic model of embedded foundation in time domain”, Earthquake Engineering Structural Dynamics, 14, 683-703.

Wolf, J. P., 1994. “Foundation Vibration Analysis Using Simple Physical Models”, Prentice Hall 1996.

Wolf, J. P., 1997. “Spring-Dashpot-Mass models for foundation vibrations”, Earthquake Engineering Structural Dynamics, 26, 931-949.

Wu, W. H., and Chen, C. Y. 2001. “Simple lumped-parameter models of foundation using mass-spring-dashpot oscillators”, Journal of the Chinese Institute of Engineers, 24(6), 681-697.

APPENDIX A

THE MAIN ANALYSIS PROGRAM "AnalysisMain"

% SSI ANALYSIS PROGRAM FOR MULTIPLE & SINGLE FREQUENCY CASES

% Loads the Earthquake data previously stored in RecordsArchive.m file

```
load Record.mat
```

% tn:The natural period (from 0.2 sec to 2.0 sec)

*% ss:Dimensionless Parameter, ss=h*wn/cs*
% hh:Dimensionless Parameter, hh=h/r0
*% mm:Dimensionless Parameter, mm=m/Ro*r0^3*
% wn:Natural Frequency
% we:equivalent frequency
% ksi:damping ratio
% nu:Poisson's ratio

```
tn = [0.2:0.2:2.0];
UUU = zeros(72,10);
```

% Gathers the structural distortion values obtained from
% the Multiple Frequency Case (Umultiple) and from the Single Frequency
% Case (Usingle)
% Calculates the Displacement Ratio (DISP) for the natural period range (tn)

```
% The values of ss, hh are to be changed for each different analysis case
% mm changes according to the hh value
% The values of ksi & nu remains the same

for j = 1:10
   Tn = tn(1,j);

   wn = 2*pi/Tn;
   ss = 1;
   hh = 5;
   mm = hh;
   ksi = 0.05;
   nu = 0.3;
   we = wn;

   [Out,Out1,Out2,Out3,Umultiple]=MTMMultiple(ss,hh,mm,ksi,wn,nu);

   [Out,Out1,Out2,Out3,Usingle]=MTMSingle(ss,hh,mm,ksi,wn,nu,we);

   DISP = Usingle./Umultiple;

   UUU(:,j) = DISP;

end

% Plots the Displacement Ratios (UUU) vs. natural period (tn)

for j = 1:72
```

```
    figure(1)
    plot (tn,UUU(j,:),'k.');
    axis([0.0 2.2 0.85 1.1]);
    xlabel('Period T_n (sec)');
    ylabel('Displacement Ratio (u(\omega_n)/u(\omega))');
    hold on;

end

% Calculates the mean values and of the displacement ratios for each
% natural period value
% Calculates the standard deviation values (+-2sigma) of the
% displacement ratios for each natural period value

for z=1:length(tn);

 AVE(z,1)=mean(UUU(:,z));
 AVE(z,2)=std(UUU(:,z));
 AVE(z,3)=AVE(z,1)-2*(AVE(z,2));
 AVE(z,2)=AVE(z,1)+2*(AVE(z,2));

 MEAN(z,1)=AVE(z,1);
 SIGM(z,1)=(AVE(z,2)-AVE(z,1))/2;

end

% Plots the lines of mean and standard deviation on top the
% previous plot of the displacement ratios vs. natural period
```

```
figure(1)
plot(tn,AVE(:,1),'k')
plot(tn,AVE(:,2),':k')
plot(tn,AVE(:,3),':k')
```

THE ROUTINE "MTMMultiple"

```
% ROUTINE FOR MULTIPLE FREQUENCY ANALYSIS OF MTM SYSTEM

function [Out,Out1,Out2,Out3,Umultiple]=MTMMultiple(ss,hh,mm,ksi,wn,nu);

% Uses the Earthquake Records data

load NDT.txt
load Record.mat

j=0;

% Executes a loop for 72 Earthquake Records
% Acceleration values (Acc) are from the corresponding EQ Data for the loop
% Uses Routine "Multiple"

Umultiple = zeros(72,1);

for z=1:72;

   j=j+1;
```

```
   N=NDT(2,z);
   dt=NDT(1,z);
   Acc=A1(:,z);
   [Out]=Multiple(N,dt,Acc,ss,hh,mm,ksi,wn,nu);

% Out1:Displacement of mass
% Out2:Displacement of foundation
% Out3:Displacement of system due to Rocking

   Out1=Out(:,1);
   Out2=Out(:,2);
   Out3=Out(:,3);

% Umultiple : The maximum absolute values of the structural displacement
% for the case of multiple frequency

   Umultiple(z) = max(abs(Out1));

end
```

THE ROUTINE "Multiple"

% ROUTINE FOR MULTIPLE FREQUENCY ANALYSIS PROGRAM (MTMMultiple.m)

```
% N:Number of Data Points
% dt:Data interval
% A1:Earthquake Acceleration Values (from :RecordsArchive.m file)
```

```
% ss:Dimensionless Parameter, ss=h*wn/cs
% hh:Dimensionless Parameter, hh=h/r0
% mm:Dimensionless Parameter, mm=m/Ro*r0^3
% wn:Natural Frequency

% Transforms the acceleration values from A1 to the frequency
% domain with the use of the Fast Fourier Transform (fft)

function [Out]=Multiple(N,dt,A1,ss,hh,mm,ksi,wn,nu);

N2=2^(ceil(log2(N)));
X=fft(A1,N2);
Out=zeros(N2,3);

% Calculates the dimensional coefficients gam0, gam1, mu0 & mu1
% of MTM Model, for horizontal & rocking motions (Table 2.1)

gam0=0.78-0.4*nu;
gam1=0.42-0.3*(nu^2);
mu1=0.34-0.2*(nu^2);

% Dynamic Coefficient General Form: S(a0)=K*[k(a0)+i*a0*c(a0)]
% k(a0) & c(a0) are dimensionless spring and damping coefficients
% Calculates the horizontal spring and damping dimensionless
% coefficients ka0h & ca0h (2.13.a & 2.13.b)
% Calculates the rotational spring and damping dimensionless
% coefficients ka0r & ca0r (2.13.c & 2.13.d)
% W(n) is the changing frequency of the earthquake record
% a0, the dimensionless frequency (2.12)
```

```
for n=1:N2/2+1
W=2*pi*(n-1)/dt/N2;
a0=(ss*W)/(hh*wn);
ka0h=1;
ca0h=gam0;
ka0r=1-(mu1*(a0^2)/(1+((mu1^2)*(a0^2)/(gam1^2))));
ca0r=(mu1/gam1)*(mu1*(a0^2)/(1+((mu1^2)*(a0^2)/(gam1^2))));

% Calculates the static stiffness coefficients for horizontal
% motion Kh (2.11.a divided by m)
% Calculates the static stiffness coefficients for rotational
% motion Kr (2.11.b divided by m*hh^2)

Kh=8*hh^2*wn^2/((2-nu)*mm*ss^2);
Kr=8*wn^2/(3*(1-nu)*mm*ss^2);

% Calculating the terms of the matrix of 2.8
% Using the changing frequency W and natural frequency wn

S1 =wn^2+wn*2*i*W*ksi-W^2;
S2 =Kh*(ka0h+i*a0*ca0h)-W^2;
S3 =Kr*(ka0r+i*a0*ca0r)-W^2;
ST=[S1 -W^2 -W^2 ; -W^2 S2 -W^2 ; -W^2 -W^2 S3];

% Calculates Outcome (Out (three displacement values, including structural
% distortion value)

Y=-[1;1;1]*X(n);
```

```
Out(n,1:3)=(ST\Y)';
end

for n=1:N2/2-1
Out((N2/2+1+n),1:3)=conj(Out((N2/2+1-n),1:3));
end

% Tranforms the displacement values back to time domain with the use of
% the Inverse Fast Fourier Transform (ifft)

Out=ifft(Out);
```

THE ROUTINE "MTMSingle"

```
% ROUTINE FOR SINGLE FREQUENCY ANALYSIS OF MTM SYSTEM

function [Out,Out1,Out2,Out3,Usingle]=MTMSingle(ss,hh,mm,ksi,wn,nu,we);

% Uses the Earthquake Records data

load NDT.txt;
load Record.mat;

j=0;

% Executes a loop for 72 Earthquake Records
% Acceleration values (Acc) are from the corresponding EQ Data for the loop
% Uses Routine "Single"
```

```
Usingle = zeros(72,1);

for z=1:72;

   j=j+1;
   N=NDT(2,z);
   dt=NDT(1,z);
   Acc=A1(:,z);
   [Out]=Single(N,dt,Acc,ss,hh,mm,ksi,wn,nu,we);

% Out1:Displacement of mass
% Out2:Displacement of foundation
% Out3:Displacement of system due to Rocking

   Out1=Out(:,1);
   Out2=Out(:,2);
   Out3=Out(:,3);

% Usingle : The maximum absolute values of the structural displacement
% for the case of single frequency

   Usingle(z) = max(abs(Out1));

end
```

THE ROUTINE "Single"

% ROUTINE FOR SINGLE FREQUENCY ANALYSIS PROGRAM (MTMSingle.m)

```
% N:Number of Data Points
% dt:Data interval
% A1:Earthquake Acceleration Values (from :RecordsArchive.m file)
% ss:Dimensionless Parameter, ss=h*wn/cs
% hh:Dimensionless Parameter, hh=h/r0
% mm:Dimensionless Parameter, mm=m/Ro*r0^3
% wn:Natural Frequency
% we:equivalent frequency

% Transforms the acceleration values from A1 to the frequency
% domain with the use of the Fast Fourier Transform (fft)

function [Out]=Single(N,dt,A1,ss,hh,mm,ksi,wn,nu,we);

   N2=2^(ceil(log2(N)));
   X=fft(A1,N2);
   Out=zeros(N2,3);

% Calculates the dimensional coefficients gam0, gam1, mu0 & mu1
% of MTM Model, for horizontal & rocking motions (Table 2.1)

   gam0=0.78-0.4*nu;
   gam1=0.42-0.3*(nu^2);
   mu1=0.34-0.2*(nu^2);
```

```
% a0e, the equivalent dimensionless frequency (2.12), calculated with a single
% frequency value (we) instead of multiple frequency
% k(a0) & c(a0) are dimensionless spring and damping coefficients
% Calculates the horizontal spring and damping dimensionless
% coefficients ka0h & ca0h (2.13.a & 2.13.b)
% Calculates the rotational spring and damping dimensionless
% coefficients ka0r & ca0r (2.13.c & 2.13.d)
% ka0r & ca0r calculated with the use of the equivalent dimensionless frequency

   a0e =(ss*we)/(hh*wn);
   ka0h=1;
   ca0h=gam0;
   ka0r=1-(mu1*(a0e^2)/(1+((mu1^2)*(a0e^2)/(gam1^2))));
   ca0r=(mu1/gam1)*(mu1*(a0e^2)/(1+((mu1^2)*(a0e^2)/(gam1^2))));

% Dynamic Coefficient General Form: S(a0)=K*[k(a0)+i*a0*c(a0)]
% W(n) is the changing frequency of the earthquake record
% a0, the dimensionless frequency (2.12)

% Calculates the static stiffness coefficients for horizontal
% motion Kh (2.11.a divided by m)
% Calculates the static stiffness coefficients for rotational
% motion Kr (2.11.b divided by m*hh^2)

   for n=1:N2/2+1
      W=2*pi*(n-1)/dt/N2;
      a0 =(ss*W)/(hh*wn);
      Kh=8*hh^2*wn^2/((2-nu)*mm*ss^2);
```

```
    Kr=8*wn^2/(3*(1-nu)*mm*ss^2);

% Calculating the terms of the matrix of 2.8
% Using the changing frequency W and natural frequency wn

    S1 =wn^2+wn*2*i*W*ksi-W^2;
    S2 =Kh*(ka0h+i*a0*ca0h)-W^2;
    S3 =Kr*(ka0r+i*a0*ca0r)-W^2;
    ST=[S1 -W^2 -W^2 ; -W^2 S2 -W^2 ; -W^2 -W^2 S3];

% Calculates Outcome (Out (three displacement values, including structural
% distortion value)

    Y=-[1;1;1]*X(n);
    Out(n,1:3)=(ST\Y)';
  end

  for n=1:N2/2-1
    Out((N2/2+1+n),1:3)=conj(Out((N2/2+1-n),1:3));
  end

% Tranforms the displacement values back to time domain with the use of
% the Inverse Fast Fourier Transform (ifft)

  Out=ifft(Out);
```